UNCLASSIFIED

AD NUMBER
AD368628
CLASSIFICATION CHANGES
TO: **UNCLASSIFIED**
FROM: **CONFIDENTIAL**
LIMITATION CHANGES
TO: **Approved for public release; distribution is unlimited.**
FROM: **Distribution authorized to U.S. Gov't. agencies and their contractors; Administrative/Operational Use; 12 JAN 1966. Other requests shall be referred to Army Missile Command, Redstone Arsenal, AL 35809.**
AUTHORITY
USAMICOM ltr dtd 1 Feb 1974 USAMICOM ltr dtd 1 Feb 1974

THIS PAGE IS UNCLASSIFIED

GENERAL DECLASSIFICATION SCHEDULE

IN ACCORDANCE WITH
DOD 5200.1-R & EXECUTIVE ORDER 11652

THIS DOCUMENT IS:

Subject to General Declassification Schedule of Executive Order 11652-Automatically Downgraded at 2 Years Intervals- DECLASSIFIED ON DECEMBER 31, 1972

BY

Defense Documentation Center
Defense Supply Agency
Cameron Station
Alexandria, Virginia 22314

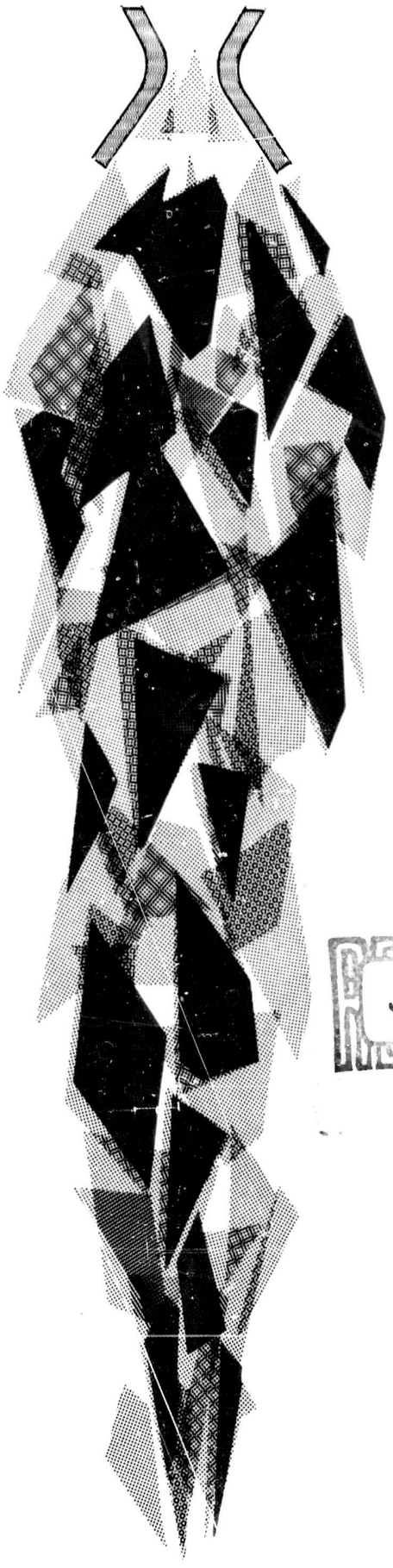
SECURITY MARKING

The classified or limited status of this report applies to each page, unless otherwise marked.
Separate page printouts MUST be marked accordingly.

THIS DOCUMENT CONTAINS INFORMATION AFFECTING THE NATIONAL DEFENSE OF THE UNITED STATES WITHIN THE MEANING OF THE ESPIONAGE LAWS, TITLE 18, U.S.C., SECTIONS 793 AND 794. THE TRANSMISSION OR THE REVELATION OF ITS CONTENTS IN ANY MANNER TO AN UNAUTHORIZED PERSON IS PROHIBITED BY LAW.

NOTICE: When government or other drawings, specifications or other data are used for any purpose other than in connection with a definitely related government procurement operation, the U. S. Government thereby incurs no responsibility, nor any obligation whatsoever; and the fact that the Government may have formulated, furnished, or in any way supplied the said drawings, specifications, or other data is not to be regarded by implication or otherwise as in any manner licensing the holder or any other person or corporation, or conveying any rights or permission to manufacture, use or sell any patented invention that may in any way be related thereto.

368628



CONFIDENTIAL

COPY NUMBER

REPORT NO. S-93

DEMONSTRATION OF A SINGLE-CHAMBER DUAL-THRUST MOTOR(U)

U. S. ARMY MISSILE COMMAND

This document contains information affecting the national defense of the United States within the meaning of the Espionage Laws, Title 18, U.S.C., Sections 793 and 794. The transmission or the revelation of its contents in any manner to an unauthorized person is prohibited by law.

DDC RECEIVED JAN 19 1966 TISIA B

DOWNGRADED AT 3 YEAR INTERVALS:
DECLASSIFIED AFTER 12 YEARS.
DOD DIR 5200.10

ROHM AND HAAS

REDSTONE RESEARCH LABORATORIES
HUNTSVILLE, ALABAMA 35807

CONFIDENTIAL

CONFIDENTIAL

ROHM & HAAS COMPANY

REDSTONE ARSENAL RESEARCH DIVISION
HUNTSVILLE, ALABAMA

Report No. S-93

DEMONSTRATION OF A SINGLE-CHAMBER DUAL-THRUST MOTOR (U)

by

B. L. Thompson

Approved by:

Louis Brown, Head
Ballistics Section

O. H. Loeffler
General Manager

Contributing Staff:

T. L. Cost

B. E. Sturgis

January 12, 1966

Contract Nos. DA-01-021 AMC-12,289 and
DA-01-021 AMC-10,037

CONFIDENTIAL

ROHM & HAAS COMPANY

REDSTONE ARSENAL RESEARCH DIVISION
HUNTSVILLE, ALABAMA

DEMONSTRATION OF A SINGLE-CHAMBER DUAL-THRUST MOTOR

ABSTRACT

A combination slotted-tube end-burning charge configuration was used to achieve a boost-to-sustain thrust ratio of about 20 in a single chamber motor assembly. The grain was cast in place with a single propellant formulation

Test firings were carried out with both plastisol nitrocellulose composite and HC binder composite propellants containing 1% aluminum. These tests demonstrated rapid and smooth transitions from the high to the low levels of operation with pressure ratios up to 17. No indication of quenching or combustion instability occurred with transitions from over 2000 psia to as low as 120 psia.

Operational capabilities over the temperature range -40°F to +140°F were demonstrated with successful firings of the composite propellant rounds. The plastisol charges failed at temperatures of -40°F.

Motors containing both plastisol and composite propellants were successfully cycled between these temperatures and withstood extended periods of cold soaking at -40°F. Charges of both propellants were successfully subjected to acceleration forces which were by a factor of two greater than would normally be experienced in a proposed application.

The 12-lbm propellant charges of both compositions delivered more total impulse than was needed to meet the requirements for this application and the dimensional envelope was not exc- -ded.

ACKNOWLEDGMENTS

Grateful acknowledgment is due Mr. Thomas L. Cost for the stress analysis of the propellant charge configuration; and Mr. Byron E. Sturgis for the work on optimization of the nozzle expansion cone and for generating the equations for the mass, center of gravity, and pressure-time curves.

TABLE OF CONTENTS

	Page
1. INTRODUCTION	1
2. OBJECTIVES	2
3. MOTOR DEVELOPMENT	2
3.1 Grain Configuration	2
3.2 Propellant Compositions	5
3.3 Liner Formulations	8
3.4 Hardware Design	8
4. PROGRAM PLAN	10
5. RESULTS OF DUAL-THRUST MOTOR FIRINGS	11
5.1 Description of Special Instrumentation	11
5.2 Special Data Reduction Procedures	12
5.3 Ballistic Results from Motors Containing Plastisol Propellant	13
5.3.1 Reproducibility Firings at +77°F	13
5.3.2 High Temperature Firings	16
5.3.3 Low Temperature Firings	16
5.4 Ballistic Results from Motors Containing Composite Propellant	17
5.4.1 Reproducibility Firings at +77°F	17
5.4.2 High Temperature Firings	17
5.4.3 Low Temperature Firings	19
6. RESULTS OF OTHER TESTS	20
6.1 Thermal Cycling Tests	20
6.2 Acceleration Tests	21
6.3 Measurement of Temperature Rise of the Nozzle	22
6.4 Calculation of Mass, Center of Gravity and Pressure-Time Curve	23
7. FEATURES OF A FLIGHT-WEIGHT MOTOR DESIGN	23
8. CONCLUSIONS	25

Appendix A - Grain Design Calculations

Appendix B - Stress Analysis of Dual Thrust Motor

Appendix C - Testing of Nozzle Throat Inserts

Appendix D - Optimization of Nozzle Expansion Cone

Appendix E - Analysis of Pressure Level of Sustainer Operation When a Significant Mass of Liner Burns

ROHM & HAAS COMPANY

REDSTONE ARSENAL RESEARCH DIVISION
HUNTSVILLE, ALABAMA

DEMONSTRATION OF A SINGLE-CHAMBER DUAL-THRUST MOTOR

1. INTRODUCTION

An inherent disadvantage of solid propellant rocket motors is the inability to change the thrust level upon command. To overcome this difficulty and to extend the usefulness of these rocket motors for tactical applications, the propellant charge and the motor hardware are designed such that the desired thrust-time history is obtained.

An example of such an application is a missile requiring a short duration, high thrust level during the initial phase of flight and a much lower, but sustained, thrust level to overcome air drag and give a constant velocity to the target area. When boost-to-sustain thrust ratios of about 10 or more are required, two separate motor chambers have generally been used despite the weight penalty and complexity of the additional hardware.

A program was undertaken at these Laboratories to investigate the feasibility of using a single-chamber rocket motor to provide booster and sustainer operations with a thrust ratio of approximately 20. The problem areas were studied in test motor firings with both plastisol nitrocellulose composite propellant and carboxy-terminated polybutadiene composite propellant. Of particular interest were the nature of the transition between high and low pressure burning, the combustion stability at relatively low sustainer pressures, and the hardware requirements.

2. OBJECTIVES

The general objectives of this effort were the extension of knowledge and experience related to the performance of single-chamber, two-level-thrust rocket motors using case-bonded, end-burning sustainer charges. Special emphasis was placed on demonstrating a boost-to-sustain thrust ratio of 20 with thrust-time parameters of 1000 lbf-1.5 sec for the booster and 50 lbf-21.5 sec for the sustainer. The following specifications provided guidelines for the design of the test motor hardware and propellant charges, and for setting up the test conditions:

(1) A propellant charge mass of approximately 12 lbm.

(2) A propellant charge outer diameter of 4 to 6 inches.

(3) An internal motor length, including the nozzle, of 20 inches or less.

(4) Operating capabilities over a temperature range of -40°F to +140°F.

(5) A booster thrust of not less than 600 lbf at -40°F and a sustainer thrust of not greater than 75 lbf at +140°F.

The relative merits of both plastisol nitrocellulose composite propellant and carboxy-terminated polybutadiene composite propellants were to be evaluated for this application.

3. MOTOR DEVELOPMENT

3.1 Grain Configuration

A variety of booster/sustainer grain combinations and designs were possible which utilized a single chamber and nozzle and a case-bonded, end-burning sustainer charge. Configurations containing separate booster and sustainer charges were considered and certain advantages were noted. For example, a different propellant composition could be used in each charge thereby allowing a choice of burning rates and/or specific impulses which, in turn, would offer latitude and

simplicity to the grain design. A design using separate charges would minimize thermal stresses and strains at high operating pressures. The undesirable characteristics include poorer ballistic reproducibility, especially if a restrictor material were necessary to control the progressivity of the burning surface, and the greater time and expense required to produce the charges.

Since manufacturing simplicity and ballistic reproducibility were primary considerations, a single-grain, cast-in-place propellant charge design was selected to demonstrate this concept. Calculations showed that the desired thrust-time parameters could be achieved within the dimensional requirements of the envelope. The grain configuration was a slotted-tube booster charge in tandem with a solid end-burning sustainer charge. The outside diameter of the propellant charge was arbitrarily fixed at 5.50 inches to permit static tests to be performed in available 6.0-inch I. D. motor hardware. (A liner thickness of 0.25 inch provided thermal protection of the case during the long burning time of the sustainer charge.)

The progressivity ratio of the booster surface area was easily controlled by the number and length of the slots. A 0.5-inch fillet radius at the forward end of the booster port was necessary to prevent excessive strains from being imposed in this area by temperature conditions and chamber pressure. The sliver fraction of the booster, a result only of the fillet at the forward end, was insignificant.

The plastisol propellant charge (Fig. 1) was 11.06 inches in length and weighed 12.0 lbm. Three slots, 2.7 inches in length, were required for an almost neutral surface-web history for the booster. Since the composite propellant has a lower burning rate at the booster pressure level, a thinner booster web was needed. The overall length of the composite charge (Fig. 2) was 12.80 inches, and the weight was 12.0 lbm. Four 2.7-inch slots were required for an acceptably neutral booster surface-web history.

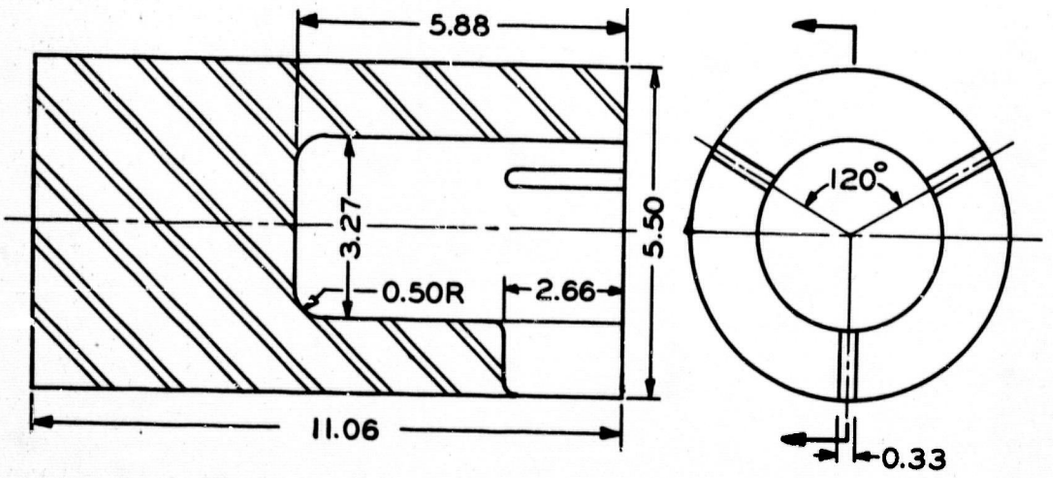


FIG. 1 GRAIN DESIGN FOR PLASTISOL PROPELLANT.

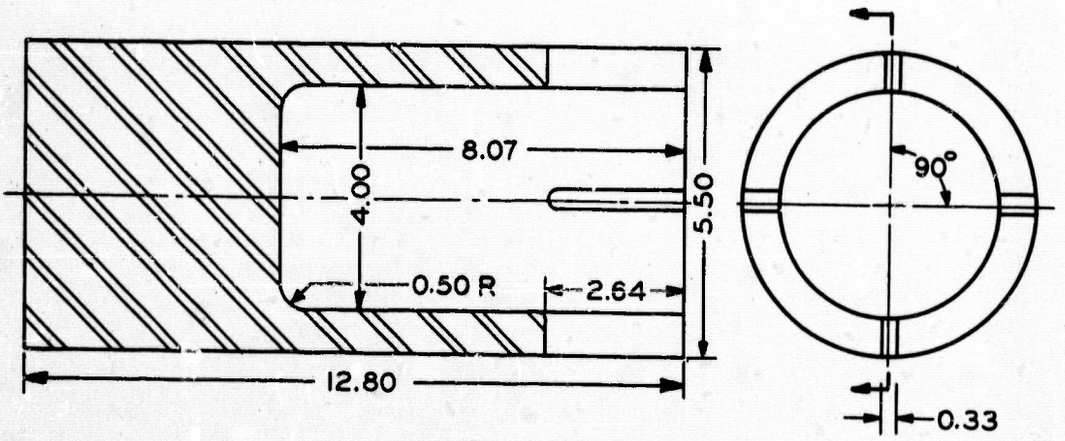


FIG. 2 GRAIN DESIGN FOR COMPOSITE PROPELLANT.

The flat forward end of the sustainer charge was not bonded to the motor head cap; instead, it was coated liberally with a lubricating grease before the head-cap was assembled to the motor. The excess grease was forced out a port in the head and the port was then plugged. The grease inhibited the head surface and provided hydrostatic support during the firing (See Fig. 5). This technique provided substantial end relief and resulted in much lower strain conditions in the head-end area.

Details of the grain design calculations are given in Appendix A and a stress analysis of the configuration is given in Appendix B.

3.2 Propellant Compositions

In order to minimize the buildup of aluminum oxide in the nozzle throat during the low-pressure sustainer operation, plastisol composition, RH-P-163, and polybutadiene composition, RH-C-27, were selected. These formulations contain 1% powdered aluminum and also produce a minimum of smoke in the exhaust gases (Table I).

Calculations showed that pressure levels of 2650 psia for the booster and 200 psia for the sustainer would produce the required 20 to 1 thrust levels for the plastisol propellant; pressures of 3000 psia and 200 psia would be needed with the composite propellant.

Burning rate vs. pressure curves for the two compositions were obtained from 2C1.5-4.0 motor firings. The rates for RH-P-163 were 0.20 in/sec at 200 psia and 0.74 in/sec at 3000 psia; the rates for RH-C-27 were 0.175 in/sec at 200 psia and 0.48 in/sec at 3000 psia (Figs. 3 and 4). Some experimental ballistic data and calculated theoretical data for these compositions are given in Table II along with mechanical properties of each propellant at three temperatures.

Table I

Composition of Propellants

Ingredients (Wt. %)	RH-C-27	RH-P-163
ZL434[a]-MAPO[b]-ERLA[c]	9.90	--
Ammonium perchlorate	84.00[d]	44.00[e]
Aluminum	1.00	1.00
Dioctyl adipate	5.00	--
Iron linoleate	0.10	--
Double base powder	--	16.67
Triethylene glycol dinitrate	--	37.33
Resorcinol	--	1.00

[a] Carboxyl-terminated polybutadiene polymer, Thiokol Chemical Corporation, Trenton, New Jersey.
[b] Tris[1-(2-methyl)oziridinyl]phosphine oxide, International Chemical Company, Newark, New Jersey.
[c] Trifunction epoxide, Bakelite Division of Union Carbide Chemical Company, New York, New York.
[d] The oxidizer was a blend of the following particle sizes: 15% 15μ, 35% 180μ, and 50% 350μ.
[e] The mean particle size of the oxidizer was 180μ.

Table II

Characteristics of Propellant Compositions

Ballistics Properties	RH-C-27			RH-P-163		
K_{1000}	345			255		
$\bar{r}_b$ at 1000 psia, in/sec	0.32			0.43		
Pressure exponent	0.37			0.48		
I_{sps}, lbf-sec/lbm	238.0			240.0		
Selected Theoretical Properties						
Chamber temperature, °K	2847			2935		
Exhaust temperature (equilibrium), °K	1347			1428		
Exhaust temperature (frozen), °K	1270			1340		
I°_{sps}, lbf-sec/lbm	243.8			246.0		
Physical Properties	Temperature			Temperature		
	-40	+77	+140	-40	+77	+140
Maximum stress, psia[a]	94	40	34	285	34	27
Maximum strain, %	6	14	15	11	19	20
Density, lbm/in^3	0.060			0.059		

[a] ICRPG specimen (die cut)

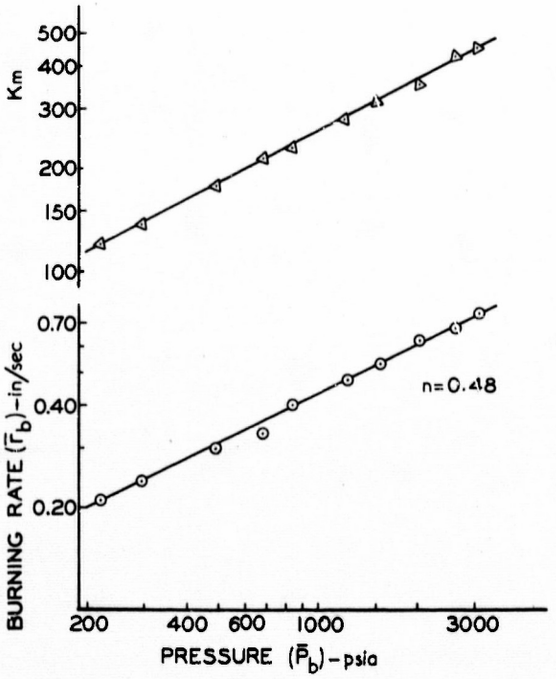


FIG. 3 P-K-r DATA FOR RH-P-163cc (PLASTISOL).

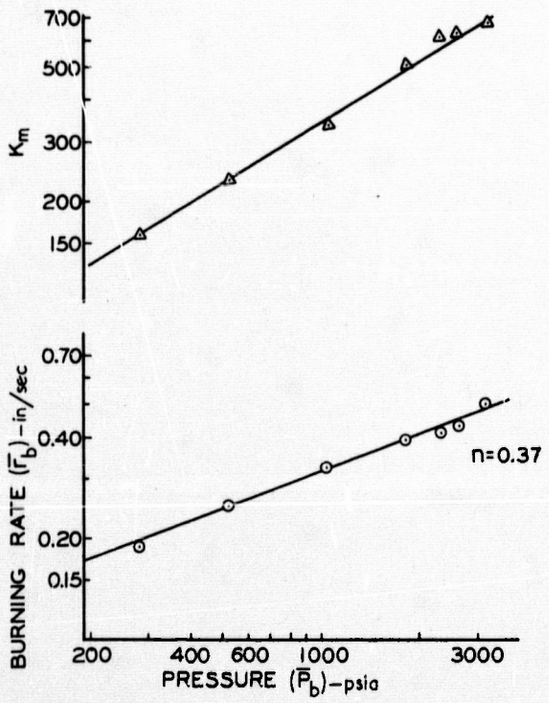


FIG. 4 P-K-r DATA FOR RH-C-27 (COMPOSITE).

3.3 Liner Formulations.

The propellant charges were cast-in-place (case-bonded) in 6-inch I. D. motor cases which were lined with 0.25 inch of liner. PL-33 liner was used for RH-P-163 propellant and CL-1 liner was used for RH-C-27 propellant. These liner formulations are given in Table III. The liners were cast into the cases using special fixtures.

Table III

Composition of Liners

Ingredients (Wt. %)	CL-1	PL-33
ZL434 binder[a]	55.0	---
Thermax[b]	22.5	---
Titanium dioxide	22.5	---
Hysol epoxy resin 2039[c]	---	20.4
Hysol hardener 3579[c]	---	26.6
Triethylene glycol dinitrate	---	23.0
Cellulose acetate powder	---	8.0
Asbestos powder	---	20.0
DMP-10[d]	---	2.0

[a] Carboxyl-terminated polybutadiene polymer, Thiokol Chemical Corporation, Trenton, New Jersey.
[b] Trademark for thermatomic carbon, R. T. Vanderbilt Co., Inc., 230 Park Avenue, New York, New York.
[c] Hysol Corporation, Olean, New York.
[d] Trademark for dimethylaminomethyl-substituted phenols, Rohm and Haas Company, Philadelphia, Pennsylvania.

3.4 Hardware Design

High-pressure 6-inch test motors, routinely used at these Laboratories, were used for these firings. A special aft-end adapter was made to hold 2-inch nozzle hardware and permit pressure measurements at the converging face. The complete motor assembly is shown in Fig. 5.

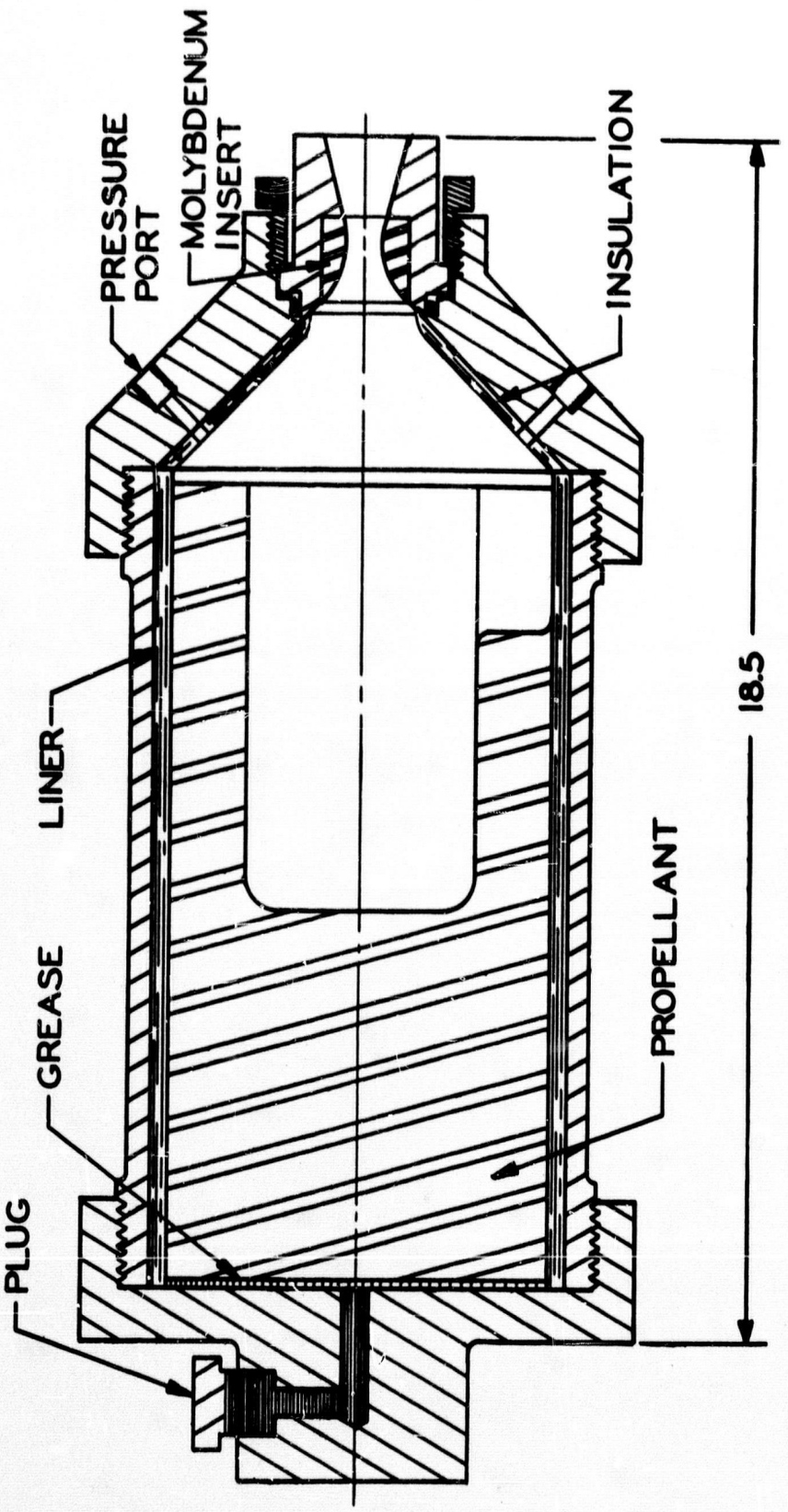


FIG. 5 MOTOR ASSEMBLY FOR DUAL THRUST ROUNDS.

Some preliminary tests were made with nozzles containing carbon inserts; the throat areas enlarged approximately 40% as a result of erosion during 1.5 seconds of operation at the booster pressure (Appendix C). From these tests it was decided that throat inserts of molybdenum would be required to withstand the high booster pressure and long sustainer burning time. Negligible erosion occurred with the molybdenum inserts.

The nozzle throats were sized according to grain design calculations. However, because of the two pressure levels obtained with these motors, a special problem existed with regard to nozzle expansion ratio. A study was carried out to determine the best expansion ratio to be used. The results showed that a compromise between under-expansion during boost and overexpansion during sustain was the most advantageous for this application (Appendix D) and an expansion ratio of about 5 was used.

4. PROGRAM PLAN

In order to obtain as much data as possible from a limited number of rounds, an eighteen-motor test program was set up for each propellant. In this program, motors were to be fired at three conditioning temperatures, cycled at high and low temperatures, and subjected to acceleration tests on a centrifuge. Since several propellant batches were necessary for obtaining the required number of rounds for this program, the motors were assigned so that both batch-to-batch and in-batch variation would be obtained (Table IV).

Table IV

Program Plan for Dual-Thrust Motors

	Number of Rounds	
	Plastisol	Composite
Rounds per propellant batch	6	3
Number of batches	3	6
Cycle at -40° F and +140° F	5	5
Acceleration test	2	3
Fire at -40° F	3	3
Fire at +140° F	3	3
Fire at +77° F	5	5
Total rounds	18	18

5. RESULTS OF DUAL-THRUST MOTOR FIRINGS

5.1 Description of Special Instrumentation

Since these motors operate at two widely different levels of pressure and thrust, special instrumentation was required to measure both levels of operation to the desired degree of accuracy. To obtain thrust measurements, two load cells, a 2000 lbf cell for measuring the booster thrust and a 200 lbf cell (equipped with an overload protection device)for measuring the sustainer thrust, were coupled in series. During booster operation, the 200 lbf cell was bottomed in its support frame. As the thrust decayed to approximately 125 lbf, this load cell began recording the thrust output of the sustainer.

A 5000 psig pressure gauge and a 500 psig gauge were used to measure the two levels of pressure. The 500 psig gauge was protected during booster operation with an inline valve between the gauge and motor. At a pre-set time after booster burn-out the valve was opened thus allowing this gauge to measure the sustainer pressure. Fig. 6 shows the arrangement of the motor and gauges on the firing stand.

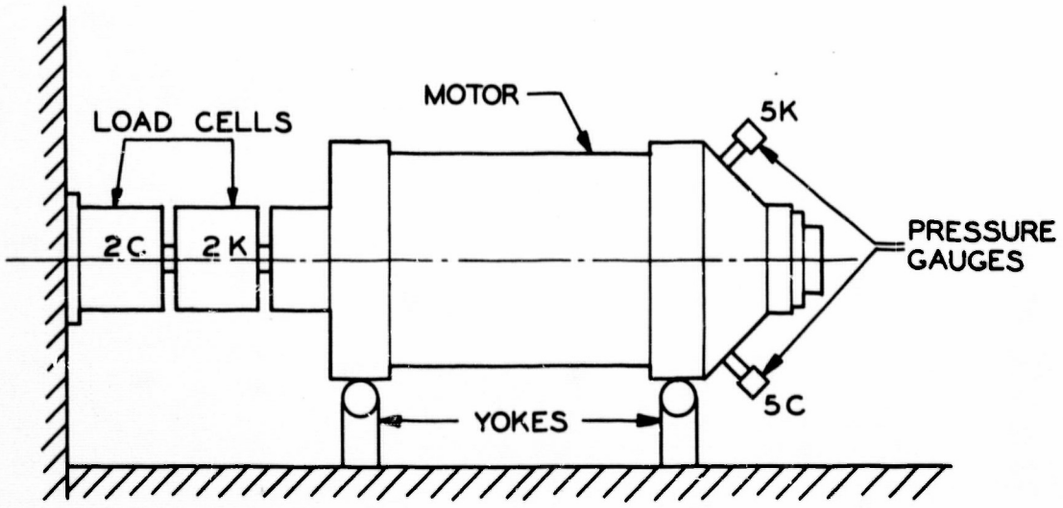


FIG. 6 THRUST STAND ASSEMBLY FOR DUAL THRUST MOTOR.

5.2 Special Data Reduction Procedures

Data reduction of the two-level pressure and thrust curves was complicated by the transition from booster to sustainer operation. Of primary interest from these rounds were the average thrust levels during the booster and sustainer burning times and the reproducibility of the transition period.

The transition phase was defined as the interval beginning at booster burnout and ending at a point tangent to normal sustainer operation. A representative thrust-time curve showing the different phases of operation is given in Fig. 7.

The other parameters were calculated using standard procedures and definitions.

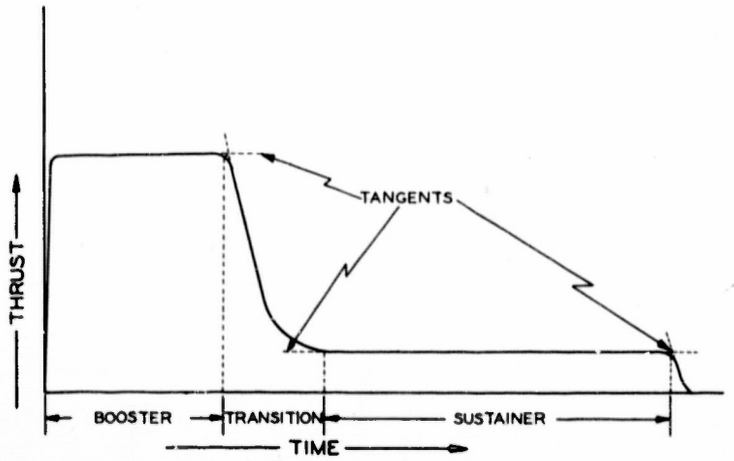


FIG. 7 REPRESENTATION OF THRUST-TIME CURVE SHOWING DIFFERENT PHASES OF OPERATION.

5.3 Ballistic Results From Motors Containing Plastisol Propellant

5.3.1 Reproducibility Firings at +77°F

Five rounds were conditioned and fired at +77°F to determine the reproducibility of the thrust-time parameters and the transition phase with RH-P-163 propellant. All rounds functioned normally. The high boost phase was followed by a sharp and smooth transition to the low sustain level; no indication of quenching or unstable combustion occurred during any part of the shot. Typical thrust-time curves are shown in Fig. 8.

The average thrust levels during boost were strongly influenced by ignition pressure and the time to reach equilibrium burning. Slow ignition resulted in the lower average thrust values ($\overline{F_b}$) obtained with Round Nos. 5083 and 5114 (Table V). Some experimentation with the igniter and nozzle closure system was necessary to obtain the desired thrust rise time of 20 msec. or less. A 15-gram jellyroll igniter and a cone-shaped ethyl cellulose closure gave good ignition results (Fig. 9).

The booster thrust-time parameters were quite close to the design values of 1000 lbf. and 1.5 sec. Since the booster thrust levels and burning times were affected by the ignition rise times, a

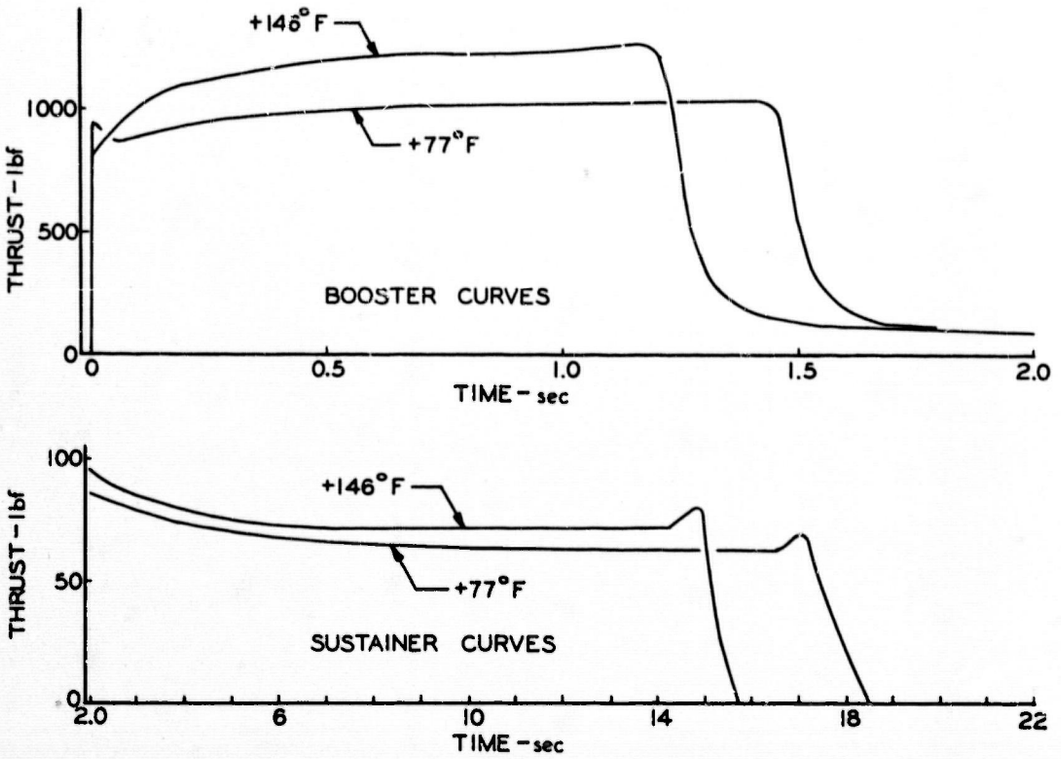


FIG. 8 THRUST-TIME CURVES FOR MOTORS WITH PLASTISOL NITROCELLULOSE PROPELLANT.

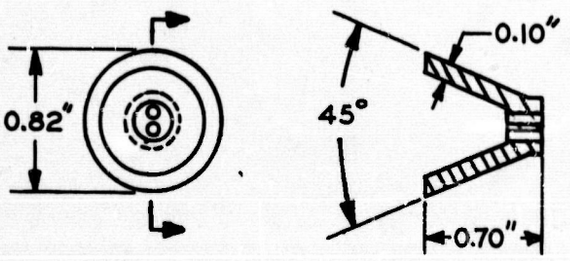


FIG. 9 ETHYL CELLULOSE NOZZLE CLOSURE (MODEL 3-O-M).

better indication of the thrust reproducibility is observed from the thrust integrals, $\int F_b$. The standard deviation of these values is less than 1%.

Table V

Ballistic Results from Rounds Containing Plastisol Nitrocellulose Propellant, RH-P-163

						Booster				
Round No.	Test Temp. (°F)	Propellant Wt. (lbm)	Weight Burned (lbm)	D_{tb} (in)	D_{te} (in)	$\bar{F}_b$ (psia)	$\bar{F}_b$ (lbf)	$\int F_b$ (lbf-sec)	t_b (sec)	I_{spd} (lbf-sec/lbm)
5083	77	11.360	12.008	0.556	0.550	2594	966	1436.82	1.487	232
5086	77	11.358	12.020	0.556	0.551	2786	994	1436.82	1.440	232
5087	77	11.433	12.075	0.556	0.550	2692	993	1450.28	1.460	234
5114	77	11.400	12.048	0.556	0.550	2536	948	1426.06	1.505	230
5113[a]	77	11.376	12.092	0.556	0.577	2450	933	1411.71	1.513	228
Average						2612	968	1432.34	1.481	231
5096	146	11.349	12.328	0.555	0.548	3296	1204	1421.26	1.180	230
5097	146	11.362	12.410	0.555	0.550	3149	1168	1412.74	1.210	228
5098	146	11.349	12.431	0.555	0.548	3292	1231	1433.88	1.165	231
Average						3245	1201	1422.62	1.185	230
5099	-40	11.384	12.021	0.555	0.545	Abnormal burning during booster.				
5100	-40	Propellant break-up and abnormal burning								
8101	-40	Overpressured at ignition and blew nozzle.								

	Transition				Sustainer					Total	
Round No.	$\bar{P}$ (psia)	$\bar{F}$ (lbf)	$\int F$ (lbf-sec)	t (sec)	$\bar{P}_b$ (psia)	$\bar{F}_b$ (lbf)	$\int F_b$ (lbf-sec)	t_b (sec)	I_{spd} (lbf-sec/lbm)	I_{spd} (lbf-sec/lbm)	I_{tot} lbf-sec
5083	770	283	114.17	0.400	234	60	918.36	15.22	166	206	2469.35
8086	786	289	112.58	0.390	213	69	1072.01	15.57	194	218	2621.41
5087	677	262	133.52	0.410	209	66	1030.03	15.22	187	216	2613.83
5114	737	261	116.27	0.445	217	66	996.97	15.17	180	211	2839.30
5113[a]	658	251	114.62	0.457	185	62	1017.37	16.41	182	210	2543.70
Average	726	269	118.23	0.420	212	65	1006.95	15.51	182	212	2557.52
5096	890	324	162.14	0.500	258	84	1109.74	13.18	192	218	2693.14
8097	797	238	126.31	0.530	205	76	1005.82	13.24	171	205	2544.87
8098	664	233	171.20	0.400	266	81	1051.66	13.19	179	214	2656.74
Average	784	265	153.21	0.477	243	80	1055.74	13.20	181	212	2631.58
5099					155	34	634.91	18.70			
5100	Propellant break-up and abnormal burning.										
5101	Overpressured at ignition and blew nozzle.										

[a]High density (1.90 g/cc) graphite nozzle insert used with this round.

The reproducibility of the transition periods was good; the average pressures, thrust integrals, and transition times were consistent (Table V).

The pressure and thrust levels of the sustainer phase were approximately 40 psig and 15 lbf., respectively, above the design values. The burning times were shortened by approximately 3 seconds as a result of the increased pressure (Table V).

The liner used with this propellant, PL-33, contained 23% of an energetic plasticizer, triethylene glycol dinitrate, and approximately 0.7 lbm. of liner was burned during each shot. An

analysis of the effect of this mass being discharged through the nozzle showed that a 33 psi increase in pressure could be expected (Appendix E). It was concluded that the higher thrust did result from the contribution of the liner mass burned.

The booster specific impulse values were calculated using the actual booster propellant weight; the weight of burned liner was included in the weight used to calculate the sustainer specific impulse. The booster values are low owing primarily to underexpansion of the gases in the nozzle while the specific impulse of the sustainer suffered because of overexpansion in the nozzle. The total specific impulse, I_{spd}, is the total impulse divided by the weight burned.

5.3.2 High Temperature Firings

Three rounds were conditioned and fired at +146°F. Normal pressure and thrust traces were obtained and transition was smooth and stable (Fig. 8). The objective of these tests was to show that the sustainer thrust level would not exceed 75 lbf. Owing to mass contribution from the motor case liner, the sustainer thrust level was higher than desired. An average of 1.04 lbm of liner burned with these rounds as opposed to 0.70 lbm for the +77°F firings. The sustainer thrust averaged 80 lbf; however, it would have been well below the 75 lbf maximum value if no mass contribution from the liner had occurred.

5.3.3 Low Temperature Firings

Three rounds were conditioned and fired at -40°F to show that the booster thrust level would not be less than 600 lbf. Round No. 5099 showed an increase in burning surface area during booster operation which resulted in an abnormal booster thrust-time curve; however, the transition period and sustainer operation appeared to be normal (Table V). Round No. 5100 experienced severe propellant break-up and abnormal burning. Apparently a crack had developed in the head-end region of the booster charge. The final round (No. 5101)

overpressured upon ignition and ejected the nozzle. The propellant charge was ejected from the motor case and burned at ambient pressure on the test bay floor.

These abnormal traces and malfunctions were probably the result of the propellant grain cracking during pressurization of the motor. No flaws were observed in the x-ray photographs before firing.

5.4 Ballistic Results from Motors Containing Composite Propellant

5.4.1 Reproducibility Firings at +77°F

Nozzles for the composite propellant rounds were sized to give pressures of 3000 psia during boost and 200 psia during sustain. The first of these rounds was fired at +77°F (Round No. 5177), and an average boost pressure of 2786 psia and a sustain pressure of 164 psia were obtained with RH-C-27 (Table VI). The average pressure levels were lower than expected; however the pressure increased during the last 20% of booster burning and was more progressive than could be accounted for with the surface-web history. The maximum pressure at booster burn-out was 3579 psia; according to K_m versus pressure relationships it should not have exceeded 3100 psia. It was concluded that the pressure exponent of the propellant began to increase slightly when the pressure exceeded 2850 psia.

The remaining rounds fired at +77°F used slightly larger nozzles which lowered the average booster pressure by approximately 500 psia; as a result the thrust levels were approximately 15% lower than the design values. Normal pressure and thrust curves were obtained with these rounds. The transition from boost to sustain was sharp, smooth, and reproducible with all rounds (Fig. 10, Table VI).

More than sufficient impulse to meet the requirements was delivered by these charges; however the distribution of the impulse needs to be improved. The booster thrust integral was low by about 11% whereas the sustainer, including transition, was about 21% high. The actual thrust levels were significantly reduced by the use of larger nozzles and the average thrust ratio was 19.3.

These tests showed that with this propellant the upper operating pressure is a limiting factor. However, smooth transition to stable combustion at pressures of 150 psia and lower will still make possible thrust ratios up to 20. The design thrust levels can be achieved at lower pressures by slightly increasing the burning rate of the propellant which would allow a larger nozzle to be used.

No significant mass contribution was made by the motor case liner.

Specific impulse values (I_{spd}) were calculated from these data using the method discussed in Section 5.3.1.

Table VI

Ballistic Results from Rounds Containing Polybutadiene Composite Propellant, RH-C-27

						Booster				
Round No.	Test Temp. (°F)	Propellant Wt. (lbs)	Weight Burned (lbs)	D_{tb} (in)	D_{ts} (in)	$\bar{P}_b$ (psia)	$\bar{F}_b$ (lbf)	$\int F_b$ (lbf-sec)	t_b (sec)	I_{spd} (lbf-sec/lbm)
5177[a]	77	11.960	12.209	0.520	0.515	2786	896	1366.28	1.525	227
5241	77	12.000	12.301	0.550	0.550	2321	842	1364.49	1.620	225
5242	77	12.012	12.272	0.550	0.548	2321	835	1532.04	1.592	220
5243	77	12.015	12.321	0.550	0.547	2284	826	1338.52	1.620	221
5514	77	11.970	12.228	0.551	0.544	2303	827	1326.50	1.605	219
Average						2307	832	1340.38	1.609	221
5291	146	12.019	12.288	0.552	0.548	2397	867	1348.77	1.555	223
5292	146	11.948	12.220	0.551	0.542	2346	850	1338.75	1.575	221
5240	146	11.991	12.270	0.552	0.549	2544	938	1350.95	1.440	223
Average						2429	885	1346.16	1.523	222
5185[a]	-40	11.988	12.246	0.520	0.514	2527	809	1546.97	1.665	224
5245	-40	11.890	12.175	0.550	0.549	2043	735	1530.61	1.810	220
5246	-40	11.880	12.255	0.550	0.548	2081	749	1363.31	1.820	225
Average						2062	742	1346.96	1.815	222

	Transition				Sustainer					Total	
Round No.	$\bar{P}$ (psia)	$\bar{F}$ (lbf)	$\int F$ (lbf-sec)	t (sec)	$\bar{P}_b$ (psia)	$\bar{F}_b$ (lbf)	$\int F_b$ (lbf-sec)	t_b (sec)	I_{spd} (lbf-sec/lbm)	I_{spd} (lbf-sec/lbm)	I_{tot} (lbf-sec)
5177[a]	994	331	147.27	0.445	164	41	1001.43	24.20	169	206	2514.98
5241	754	282	132.54	0.470	138	44	1405.91	27.46	210	220	2792.04
5242	715	256	157.21	0.615	145	40	1056.31	26.58	179	207	2545.56
5243	676	246	169.99	0.690	143	43	1148.88	26.53	194	216	2657.39
5514	907	334	148.48	0.445	142	45	1215.68	27.34	208	220	2690.66
Average	763	280	152.05	0.555	142	43	1156.69	26.98	197	216	2640.13
5291	746	292	138.76	0.475	144	48	1243.42	26.20	208	222	2750.85
5292	770	294	130.63	0.445	147	44	1139.10	26.07	192	213	2608.50
5240	761	275	143.01	0.530	140	38	983.39	25.85	165	202	2477.35
Average	759	287	137.43	0.483	144	43	1121.97	26.04	189	212	2605.56
5185[a]	957	289	137.13	0.475	157	55	896.91	27.06	150	194	2381.01
5245	655	241	118.19	0.490	120	35	1063.68	50.83	181	206	2394.29
5246	638	226	92.71	0.410	120	55	1017.67	30.94	170	202	2473.69
Average	646	254	105.45	0.450	120	34	1040.67	30.89	176	204	2416.33

[a]Values for this round are not included in the averages because of the different size nozzle used.

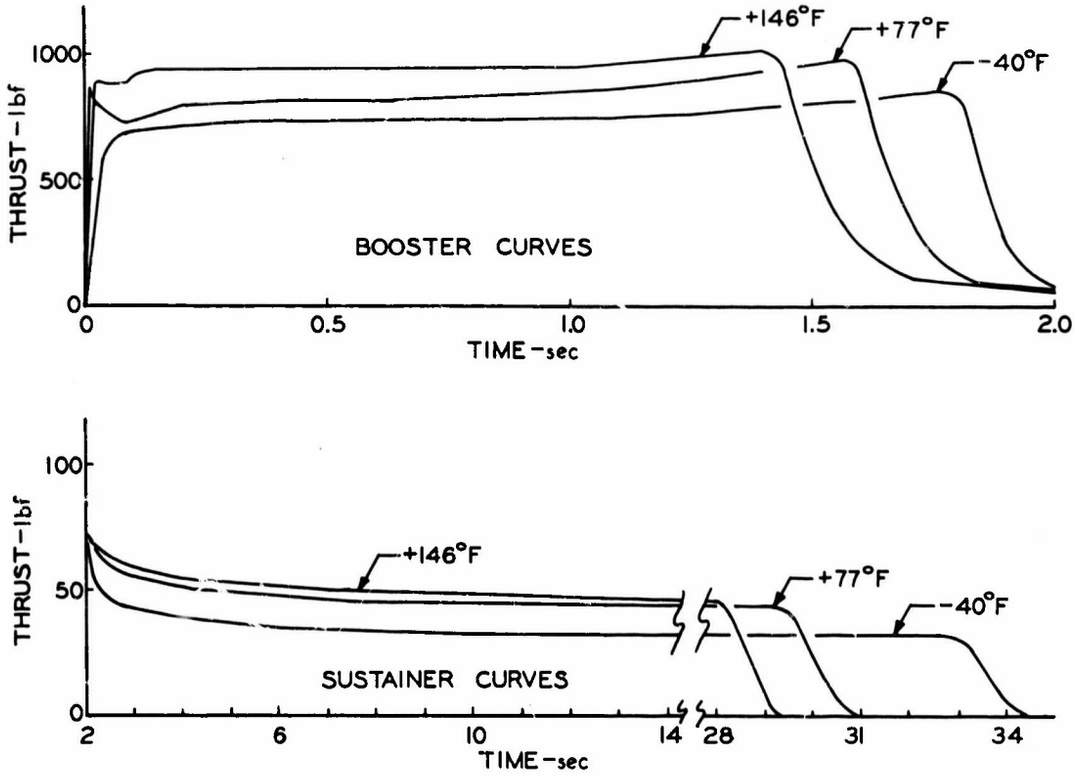


FIG. 10 THRUST-TIME CURVES FOR MOTORS WITH POLYBUTADIENE COMPOSITE PROPELLANT.

5.4.2 High Temperature Firings

Three rounds were fired at +146°F and all burned normally.giving traces similar to those of the +77°F firings (Fig. 10, Table VI). The thrust levels were only slightly higher, 6-7%, than the +77°F levels. The pressure data showed the temperature coefficient for these temperatures to be about 0.10%/°F which is typical of this type of propellant.

5.4.3 Low Temperature Firings

The first round fired at -40°F (Round No. 5183) used a nozzle originally sized for these motors, and an average pressure of

2527 psia was obtained during booster operation. Although this firing was completely normal, the remaining two rounds designated for testing at this temperature were fired with the larger size nozzles in order that data comparative with the other tests could be obtained.

As stated previously, the objective of the -40°F tests was to show that the booster thrust level would not be less than 600 lbf. Although these firings were made at lower pressures than were originally intended, the booster thrust levels averaged 742 lbf which was considerably higher than the 600 lbf value (Table VI). The sustainer pressure was quite low, 120 psig, and the sustainer impulse was correspondingly low; however, stable combustion was obtained throughout the shots.

6. RESULTS OF OTHER TESTS

6.1 Thermal Cycling Tests

Several motors from each propellant composition were subjected to thermal cycling tests at -40°F and +140°F to determine the structural integrity of the charge design. Two motors of each composition were shock-cycled, i. e., carried directly from one temperature extreme to the other without equilibrating at +77°F. Two motors each were allowed to equilibriate at +77 °F between the temperature extremes; and one motor each was soaked at -40°F for an extended period of time.

The charges were visually inspected after each half-cycle and occasionally x-rayed while at -40°F. No indication of failure was observed in the booster portion of the charges. A $\frac{1}{4}$-inch deep circumferential propellant/liner separation occurred at the head end of the solid sustainer charges of plastisol propellant after a few cycles at -40°F. The separations were not considered to be significant, since no flame would reach this area until complete burn-out. No failure occurred with the composite propellant charges. A summary of the cycling data is given in Table VII. Three rounds were fired successfully at +77°F after undergoing 10 shock cycles.

Table VII

Results from Thermal Cycling Tests

Charge No.	No. Cycles	Accumulative Days -40°F	+77°F	+140°F	Comments
Plastisol					
P-5-1[a]	10	15	0	15	A 360° propellant-liner separation occurred at the head end of the sustainer charge after two cycles. The maximum depth of separation was 1/4 to 3/8 inch.
P-17-3[a]	10	16	0	15	
P-1-1	8	28	22	16	
P-7-2	8	23	22	16	
P-13-3	0	58	0	0	
Composite					
C-3-1[a]	10	19	0	22	No failures occurred with any charge.
C-1-1	8	13	10	10	
C-4-2	8	19	14	10	
C-14-5	0	30	0	0	

[a]These rounds fired successfully after undergoing 10 shock cycles.

6.2 Acceleration Tests

Two motors of each propellant composition were subjected to acceleration tests on a centrifuge. The acceleration load was gradually increased up to a maximum of 17 g's during approximately 120 seconds and then decelerated to 0 g during approximately 60 seconds. No failure occurred at these test conditions. The acceleration load was then increased to 35 g's during approximately 165 seconds, and no failure occurred. These motors were later fired at +77°F and normal pressure and thrust curves were obtained.

In an effort to determine the load required for failure, the load on one composite motor was gradually increased to 75 g's and held for approximately 15 minutes. No failure occurred at these conditions. Since the 75 g load was the maximum available with the centrifuge and was considerably more than this motor would experience, no further tests were made.

6.3 Measurement of Temperature Rise of the Nozzle

In the actual application of this type motor it might be desirable for some guidance instrumentation and control units to be packaged around the aft end of the unit. Thus, the maximum temperature of the outside surface of the nozzle would need to be kept within an acceptable range.

The outside surface temperature of the nozzle was recorded during firing with Round No. 5113. The nozzle contained a throat insert of high density (1.90 g/cc) graphite. No attempt was made in this test to insulate the throat insert from the nozzle housing; therefore, the temperatures obtained are considerably higher than would be experienced if an insulated nozzle design were used.

Fig. 11 shows the test set up. The temperature appeared to level off at 18 seconds at 500°F (Fig. 12).

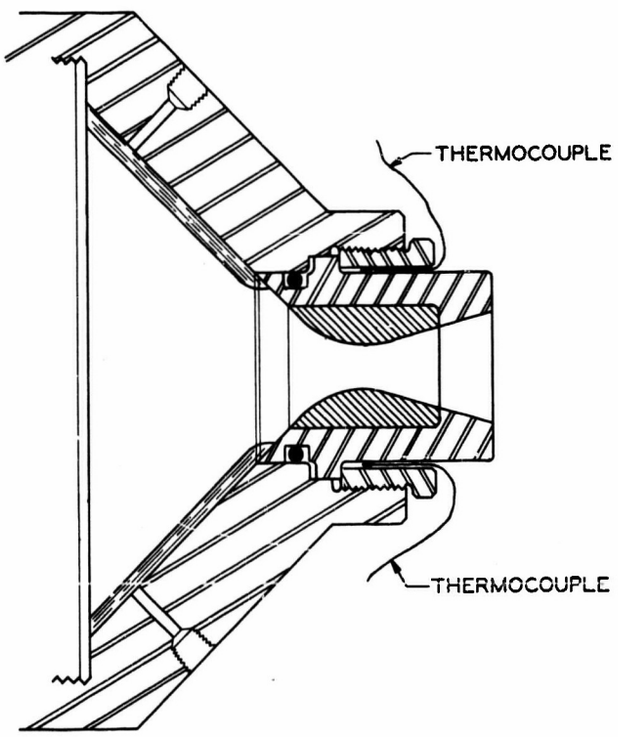


FIG. 11 NOZZLE SECTION SHOWING LOCATION OF THERMOCOUPLES.

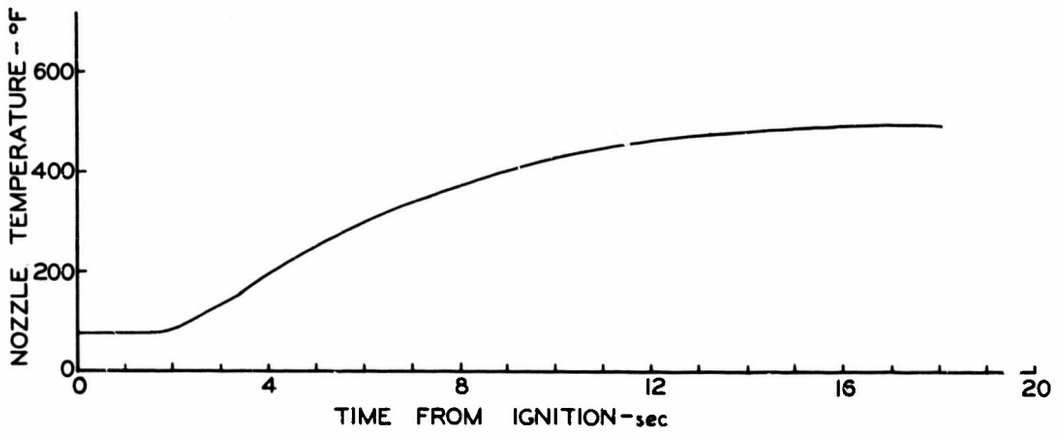


FIG. 12 OUTSIDE SURFACE TEMPERATURE OF NOZZLE CONTAINING GRAPHITE INSERT.

6.4 Calculation of Mass, Center of Gravity, and Pressure-Time Curve

Generalized equations were developed for determining the mass, center of gravity location, burning surface area, chamber pressure, burning rate and elapsed burning time as a function of consumed web for any slotted tube grain cast tandem to an end burning grain. A FORTRAN program was prepared and the values were printed out for small web increments for the composite grain (Table VIII). Equations which included pressure decay solutions during the transition period from booster chamber pressure to sustainer chamber pressure were also developed and a predicted pressure-time curve was generated for plastisol propellant. The agreement was excellent (Fig. 13).

7. FEATURES OF A FLIGHT-WEIGHT MOTOR DESIGN

All firings of the dual-thrust grains were carried out in heavy-weight static test hardware. However, the techniques needed to fabricate a flight motor are well-developed. Fig. 14 is a layout that shows the important design features.

The motor case is a high-strength steel tube with an elliptical head-end closure. A release boot at the head-end allows the grain to move freely during cure and thermal cycling. Grease may be used to provide hydrostatic support during firing, if necessary.

Table VIII

CALCULATION OF CHANGE IN MASS, CENTER OF GRAVITY, AND THE BURNING SURFACE HISTORY OF A SOLID PROPELLANT GRAIN

PROPELLANT FORMULATION COMPOSITE C27 STUHGIS 11/30/65

PROGRAM #91

R =	2.7500	ROE =	0.0600	L1 =	5.2300	L2 =	10.3200		
R4 =	1.5000	S5 =	7.0686	B =	1.2500	DELX =	0.0500		
R11 =	2.0000	R21 =	0.1650	C1 =	0.3300	L11 =	2.4800		
L31 =	4.9250	A1 =	0.5000	L51 =	4.7300	N =	4.0000		
AT =	0.2376	AR =	0.0229	NK =	0.3800	CD =	0.0065		
RGC =	83.1900	TC =	5123.0000	L? =	14.0000	LCT =	3.1000		
DELX2 =	0.0050	DELX3 =	0.2000	DELPCL =	2.0000				

	DISTANCE BURNED	TOTAL MASS	TOTAL SURFACE	XBAR	CHAMBER PRESSURE	BURNING RATE	BURNING TIME
	0.0000	12.0448	128.8611	5.1347	2091.4256	0.4184	0.1195
	0.0500	11.6417	129.9070	5.0017	2124.1867	0.4209	0.2363
	0.1000	11.2385	131.0915	4.8636	2159.5131	0.4232	0.3564
	0.1500	10.8352	132.2139	4.7196	2165.3572	0.4255	0.4740
	0.2000	10.4316	133.2735	4.5696	2213.6761	0.4275	0.5909
	0.2500	10.0284	134.2699	4.4122	2240.4319	0.4295	0.7073
	0.3000	9.8249	135.2028	4.2466	2265.9909	0.4313	0.8232
	0.3500	9.2212	136.0718	4.0717	2269.1238	0.4330	0.9367
	0.4000	8.8174	136.8767	3.8863	2311.0057	0.4346	1.0536
	0.4500	8.4134	137.6176	3.6888	2331.2152	0.4360	1.1664
	0.5000	8.0093	136.2945	3.4773	2349.7353	0.4373	1.2828
	0.5500	7.6051	138.9073	3.2495	2366.5525	0.4385	1.3966
	0.6000	7.2008	139.4563	3.0027	2381.6569	0.4396	1.5105
	0.6500	6.7960	139.9417	2.7333	2395.0423	0.4405	1.6240
	0.7000	6.3912	140.3639	2.4372	2406.7061	0.4413	1.7373
BEGIN E BURN OUT	0.7500	5.9861	140.7231	2.1086	2416.6488	0.4420	1.8504
	0.7500	5.9160	35.3916	2.0630	1946.8082	0.4072	1.8627
	0.7550	5.9073	33.6056	2.0796	1547.9645	0.3732	1.8761
	0.7600	5.8979	32.9459	2.0763	1219.0739	0.3408	1.8906
	0.7650	5.8884	32.4691	2.0728	953.6930	0.3105	1.9069
	0.7700	5.8790	32.0659	2.0693	744.6153	0.2826	1.9246
	0.7750	5.8696	31.7620	2.0659	584.2420	0.2577	1.9440
	0.7800	5.8602	31.4799	2.0625	464.7991	0.2363	1.9651
	0.7850	5.8509	31.2291	2.0591	378.5818	0.2185	1.9880
	0.7900	5.8417	31.0038	2.0557	318.2643	0.2046	2.0124
	0.7950	5.8325	30.7968	2.0524	277.2496	0.1941	2.0382
	0.8000	5.8234	30.6071	2.0491	249.9739	0.1867	2.0650
	0.8050	5.8143	30.4315	2.0458	232.0667	0.1815	2.0925
	0.8100	5.8053	30.2679	2.0425	220.3219	0.1779	2.1206
	0.8150	5.7963	30.1147	2.0393	212.5235	0.1755	2.1491
	0.8200	5.7873	29.9708	2.0360	207.2086	0.1738	2.1779
	0.8250	5.7784	29.8350	2.0326	203.4436	0.1726	2.2069
	0.8300	5.7695	29.7065	2.0296	200.6462	0.1717	2.2360
	0.8350	5.7607	29.5846	2.0264	198.4572	0.1710	2.2652
TRANSITION COMPLETE	0.8400	5.7519	29.4686	2.0233	196.6576	0.1704	2.2946
	1.0400	5.4189	27.0116	1.9044	166.6784	0.1607	3.5306
	1.2400	5.1058	26.0021	1.7936	156.6278	0.1578	4.8125
	1.4400	4.8019	25.4332	1.6865	153.0680	0.1549	6.1035
	1.6400	4.5031	25.0667	1.5813	149.5455	0.1535	7.4060
	1.8400	4.2075	24.8171	1.4774	147.1316	0.1526	8.7166
	2.0400	3.9141	24.6344	1.3743	145.3887	0.1519	10.0332
	2.2400	3.6222	24.4968	1.2718	144.0810	0.1514	11.3542
	2.4400	3.3314	24.3901	1.1697	143.0708	0.1510	12.6788
	2.6400	3.0415	24.3056	1.0679	142.2717	0.1507	14.0063
	2.8400	2.7522	24.2373	0.9665	141.6276	0.1504	15.3360
	3.0400	2.4635	24.1813	0.8652	141.1002	0.1502	16.6676
	3.2400	2.1753	24.1348	0.7641	140.6623	0.1500	18.0007
	3.4400	1.8874	24.0956	0.6631	140.2943	0.1499	19.3352
	3.6400	1.5998	24.0623	0.5623	139.9821	0.1497	20.6709
	3.8400	1.3124	24.0336	0.4617	139.7146	0.1496	22.0075
	4.0400	1.0253	24.0092	0.3612	139.4837	0.1495	23.3449
	4.2400	0.7383	23.9878	0.2609	139.2828	0.1495	24.6831
	4.4400	0.4515	23.9690	0.1613	139.1070	0.1494	26.0219
	4.6400	0.1649	23.9524	0.0652	138.9522	0.1493	27.3613

END OF PROBLEM

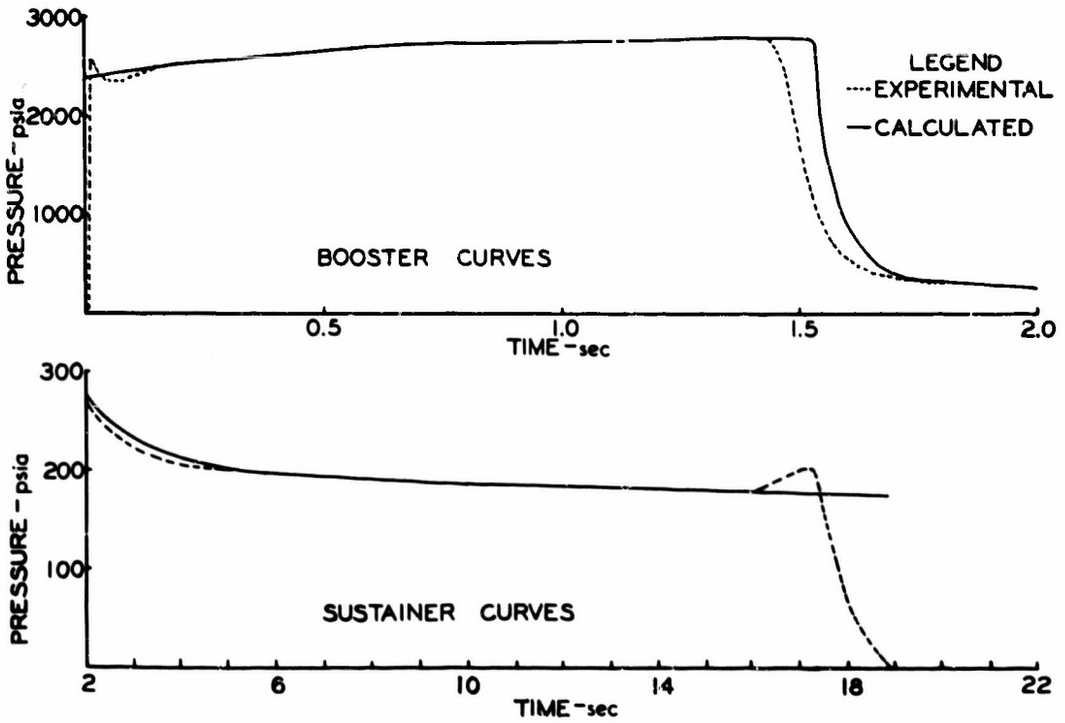


FIG. 13 COMPARISON OF EXPERIMENTAL VS. CALCULATED PRESSURE-TIME CURVE.

The motor case liner is tapered toward the forward end of the grain to allow a higher propellant loading fraction. The material is an asbestos-phenolic or asbestos-rubber material having low ablation characteristics.

The nozzle uses a molybdenum throat insert which is thermally insulated from the nozzle housing with a carbon-phenolic cloth material. The converging and diverging sections of the nozzle are also protected from overheating by a layer of ablative insulation. If the motor location in the missile is critical, a sub-sonic blast tube can be incorporated between the nozzle and motor to obtain an acceptable position.

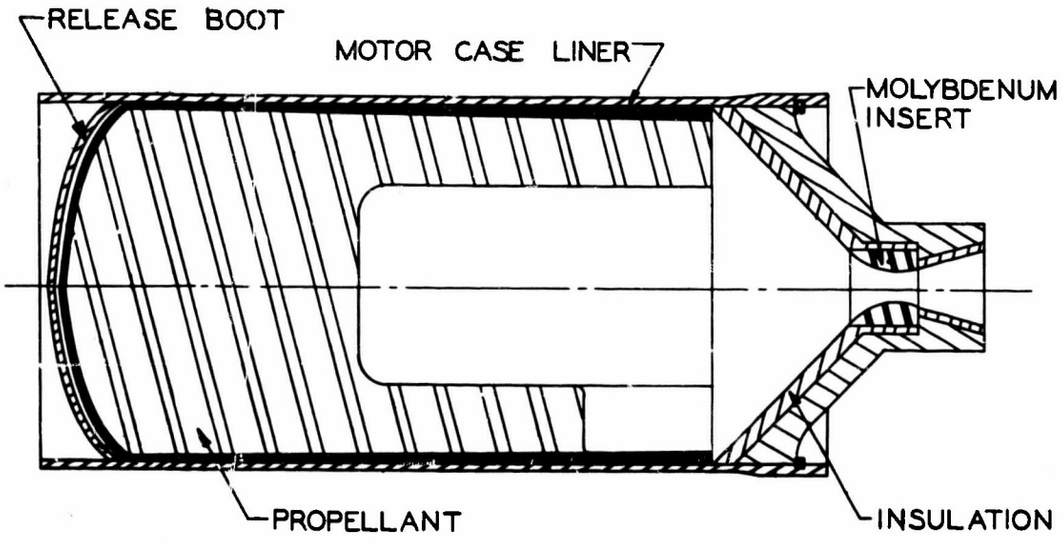


FIG. 14 FEATURES OF A FLIGHT WEIGHT MOTOR DESIGN.

8. CONCLUSIONS

A combination slotted-tube end-burning charge configuration was used to achieve a boost-to-sustain thrust ratio of about 20 in a single chamber motor assembly. The grain was cast in place with a single propellant formulation.

Test firings were carried out with both plastisol nitrocellulose composite and HC binder composite propellants containing 1% aluminum. These tests demonstrated rapid and smooth transitions from the high to the low levels of operation with pressure ratios up to 17. No indication of quenching or combustion instability occurred with transitions from over 2000 psia to as low as 120 psia.

Operational capabilities over the temperature range -40°F to +140°F were demonstrated with successful firings of the composite propellant rounds. The plastisol charges failed at temperatures of -40°F.

The structural integrity of this charge design was proven in thermal cycling tests at -40°F and +140°F. Motors containing both plastisol and composite propellants were successfully cycled between these temperatures and withstood extended periods of cold soaking at -40°F. Charges of both propellants were successfully subjected to acceleration forces which were by a factor of two greater than would normally be experienced in a proposed application.

The ballistic data from motors containing composite propellant showed thrust ratios of 20, but the thrust levels were approximately 15% lower than desired. The correct thrust levels can be easily obtained with a slightly higher burning rate propellant.

The thrust ratios of the plastisol propellant rounds were low as a result of higher-than-expected sustainer thrust levels. The high sustainer thrust was accounted for by mass contribution from the motor case liner. The PL-33 liner was selected for these tests because it was easily processed and readily available. Other liner formulations which are much less ablative are available for this propellant. The booster thrust-time parameters were very near the design values.

The 12-lbm propellant charges of both compositions delivered more total impulse than was needed to meet the requirements for this application and the dimensional envelope was not exceeded.

APPENDIX A
GRAIN DESIGN CALCULATIONS

An idealized thrust-time curve for the dual-thrust motor is shown in Fig. A-1.

The sustainer charge configuration, a solid end-burning charge, was established by the technical requirements and the charge diameter was arbitrarily fixed at 5.50 inches to permit utilization of presently available hardware. The propellant formulations were selected for this application as discussed in Section 3.2. The propellant mass required for the total sustainer impulse was determined by Eq. (A-1).

$$m_p = \frac{I_{tot}}{I_{sps} \times \frac{C_{F_{test}}}{C_{F_{std}}}} \qquad (A\text{-}1)$$

where I_{tot} = total impulse

m_p = propellant charge weight

I_{sps} = specific impulse corrected to 1000 psia chamber pressure, optimum expansion ratio at sea level pressure (14.7 psia), and 0° nozzle exit angle.

$C_{F_{test}}$ = thrust coefficient at test conditions.

$C_{F_{std}}$ = thrust coefficient at standard conditions.

The continuity equation (A-2) was used to calculate the burning rate of the sustainer charge.

$$r = \frac{\dot{m}}{\rho S} \qquad (A\text{-}2)$$

where r = burning rate, $\dot{m}$ = mass discharge rate, ρ = propellant density, and S = propellant surface area. The pressure corresponding to this burning rate was obtained from experimental data. Again the continuity equation (A-3) was utilized to determine the nozzle throat area, A_t.

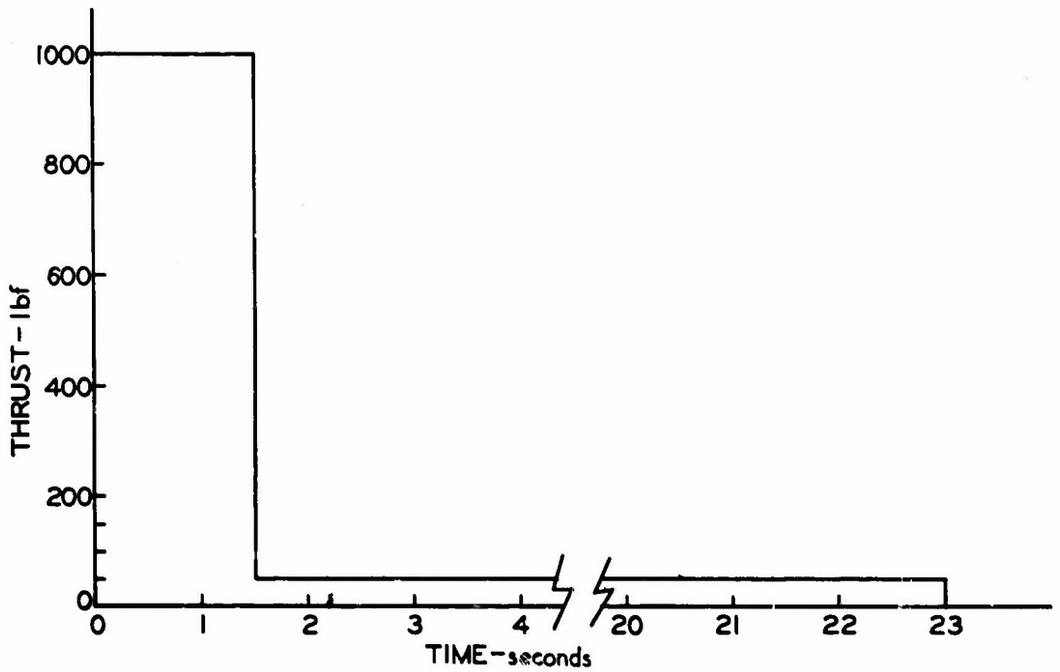


FIG. A-1 IDEALIZED THRUST-TIME TRACE.

$$A_t = \frac{\dot{m}}{C_D P_c} \tag{A-3}$$

C_D = discharge coefficient and P_c = chamber pressure.

Equations (A-1) and A-2) were used to calculate the propellant weight and burning rate of the booster charge. Since the nozzle throat area was established from sustainer calculations, the booster chamber pressure was determined from Eq. (A-4)

$$P_c = \frac{\dot{m}}{C_D A_t} \tag{A-4}$$

The surface area of the booster charge was derived from Eq. (A-5),

$$\frac{\left(\rho S c P^n\right)_b}{\left(\rho S c P^n\right)_s} = \frac{\left(C_D A_t P\right)_b}{\left(C_D A_t P\right)_s} \tag{A-5}$$

where c = burning rate constant and n = pressure exponent. The subscripts b and s represent the booster and sustainer respectively. Cancelling terms and rearranging gives

$$S_b = S_s \left(\frac{P_b}{P_s} \right)^{1-n} \qquad (A-6)$$

The booster surface areas were then calculated using techniques outlined in grain design reports.[1]

A summary of the calculated design parameters for both propellant compositions is given in Table A-I.

Table A-I

Calculated Design Parameters for Dual Thrust Motors

	Plastisol		Composite	
	Booster	Sustainer	Booster	Sustainer
Thrust, lbf	1000	50	1000	50
Burning time, sec.	1.5	21.5	1.5	21.5
Pressure, psia	2650	175	3000	200
Burning rate, in/sec	0.73	0.18	0.50	0.18
Surface area, in^2	95	25	135	25
Nozzle throat area, in^2	0.2428		0.2127	

[1] Rohm and Haas Company, "The Slotted Tube Grain Design," S-27 December 1960.

APPENDIX B

STRESS ANALYSIS OF DUAL THRUST MOTOR

Introduction

The structural integrity of the dual thrust motor propellant grain has been analyzed in regard to loads resulting from thermal shrinkage and from ignition at low temperatures. Three variations of the basic design were analyzed. Each variation has a different fillet at the bottom of the port; otherwise, the grains are identical.

The analysis was performed using the finite element method which has been programmed for computer operation for the cases of plane strain (or plane stress) and axial symmetry. This method has been widely described in the open literature.

Propellant Mechanical Properties

The propellant tested and analyzed was a nitrocellulose plastisol propellant RH-P-163 cc. The mechanical property data is presented graphically in Figs. B-1 - B-3. Fig. B-1 is a plot of the relaxation modulus of the material assuming the material is linear viscoelastic and that the strain is applied at a constant rate. The modulus in Fig. B-1 is shown plotted against reduced time. The shift function (A_T) for this material is shown in Fig. B-2 as a function of temperature. The failure limits of the propellant are shown in Fig. B-3 where the maximum allowable stress and strain are shown as functions of reduced time.

The coefficient of cubical expansion of the propellant was estimated to be $\alpha_v = 2.26 \times 10^{-4} \frac{in^3}{in^3 - °F}$. The bulk modulus of the propellant was assumed to be 350,000 psi, a value typical for most solid propellants. The grain was assumed to be encased in an aluminum cylinder with a tensile modulus of 10.7×10^6 psi.

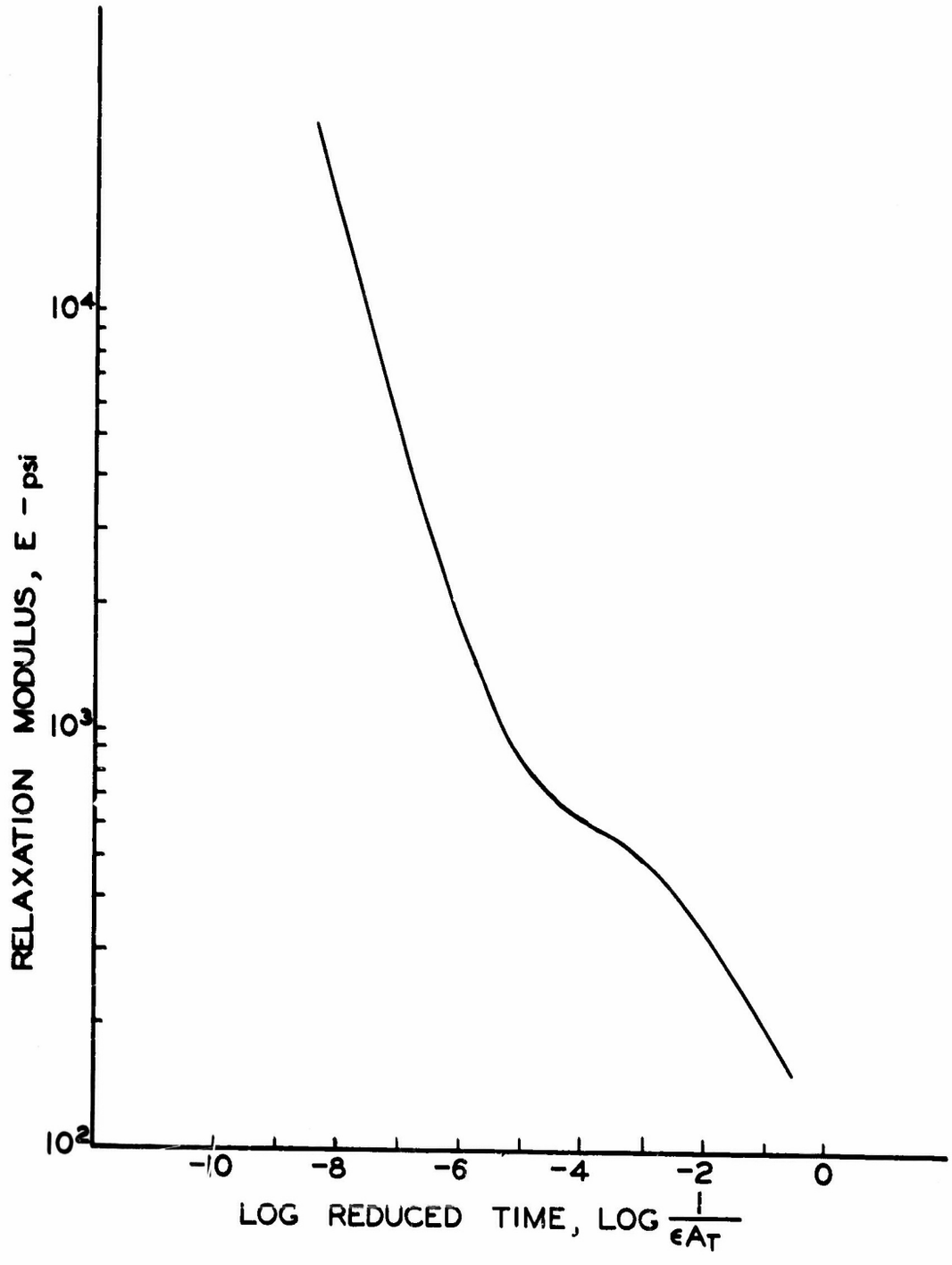


FIG. B-1 RELAXATION MODULUS VERSUS REDUCED TIME FOR RH-P-163cc PROPELLANT (A_T = 1 at 75°F).

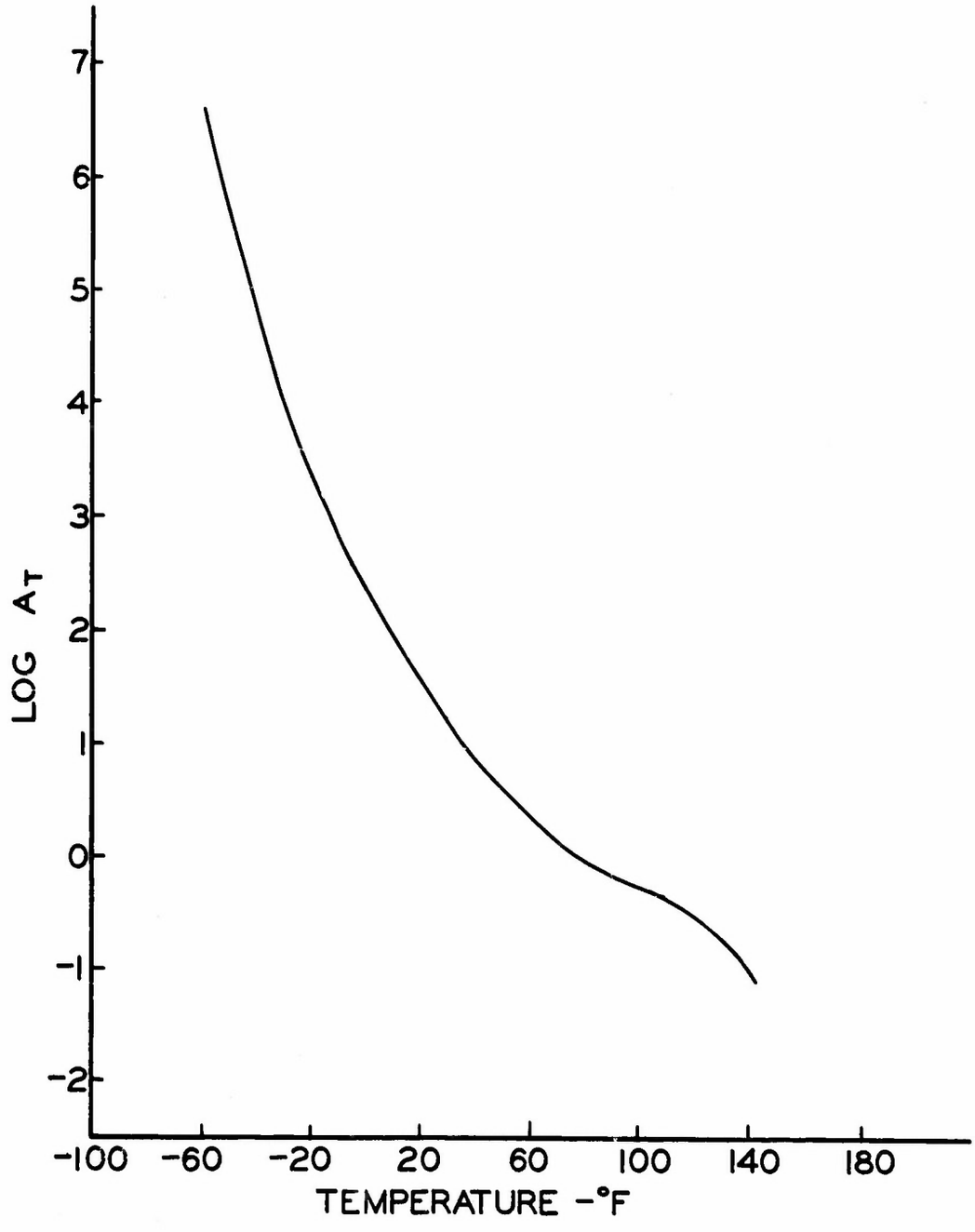


FIG. B-2 SHIFT FUNCTION VERSUS TEMPERATURE FOR RH-P-163cc PROPELLANT.

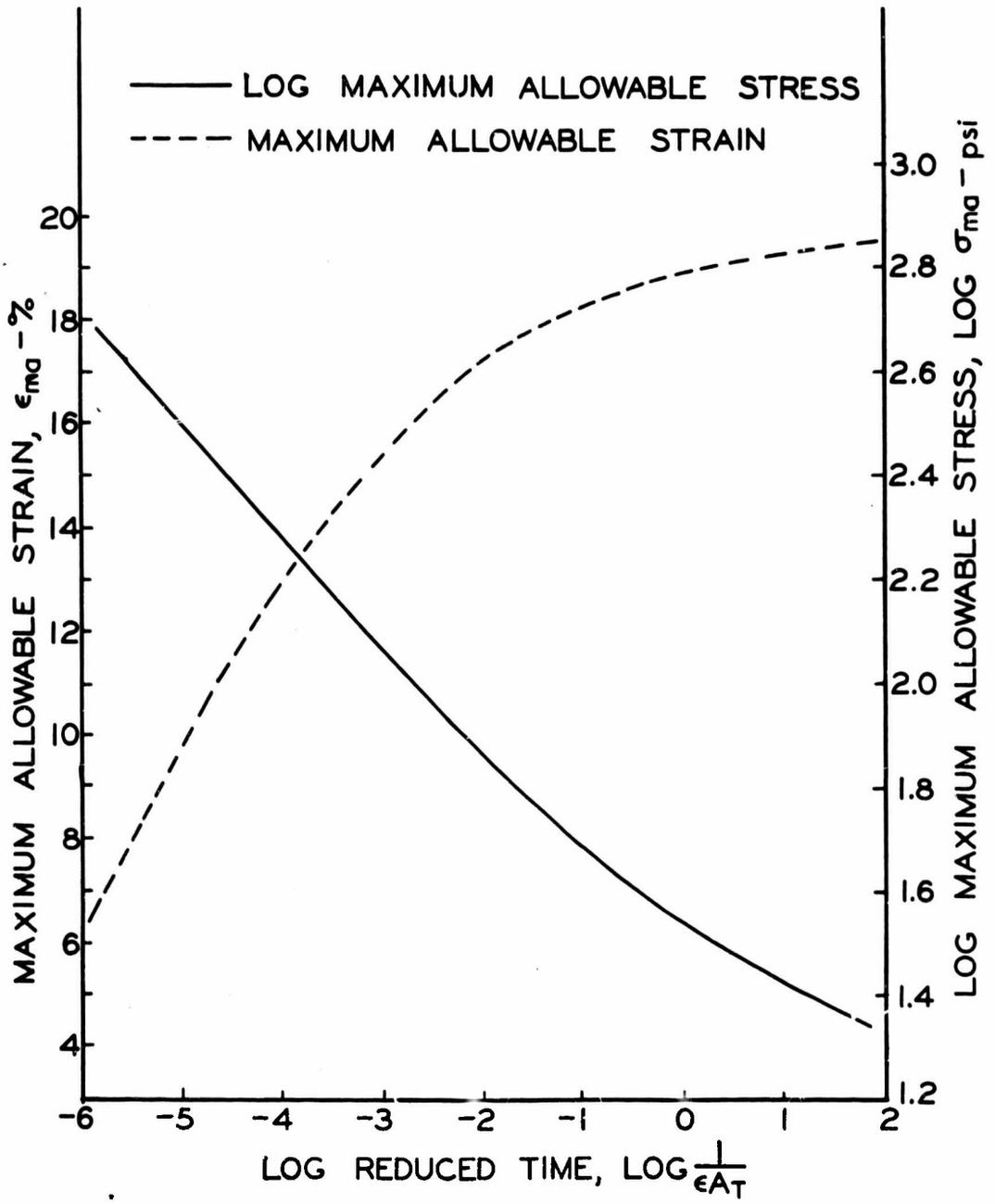


FIG. B-3 FAILURE LIMITS IN UNIAXIAL EXTENSION FOR RH-P-163cc PROPELLANT (A_T = 1 at 75°F).

Results of Analysis

As mentioned in the Introduction, three variations of the basic grain design were analyzed. The three variations designated as variations A, B, C had fillet radii of 0.25-, 0.5-, and 0.75-inches, respectively. Since these variations differ only in the radius of the fillet at the bottom of the port, the results of the different analyses would be expected to differ only in the local area surrounding the fillet. Therefore, results for the three variations will be presented separately only for the fillet area.

By examining a diagram of the motor, it can be seen that slots are present in the aft end of the motor which provide for additional burning area. The stress or strain distributions around these slots have not been evaluated for two reasons. First, it does not appear that the configuration of the slots would produce conditions as critical as other areas of the motor which are being analyzed in detail. Secondly, the slots cannot easily be taken into account in using the finite element method due to the non-axisymmetry nature of the resulting grain.

Operating conditions require the motor to be cycled between +140°F and -40°F and the chamber pressure upon ignition is specified to be 3000 psi. An analysis was made of the thermal shrinkage problem resulting from the thermal cycling and this analysis is described first. Following this, the analysis of the pressurization problem at low temperature is described.

1. Thermal Shrinkage Analysis

The motor was assumed to be cooled to -40°F from +80°F over a period of two hours. Using the above values for the material properties, the finite element method was used to determine the stresses, strains, and displacements for the configuration with a 0.25-inch fillet radius. Fig. B-4 gives the maximum normal stress and strain distributions in the body analyzed. The figures are intended

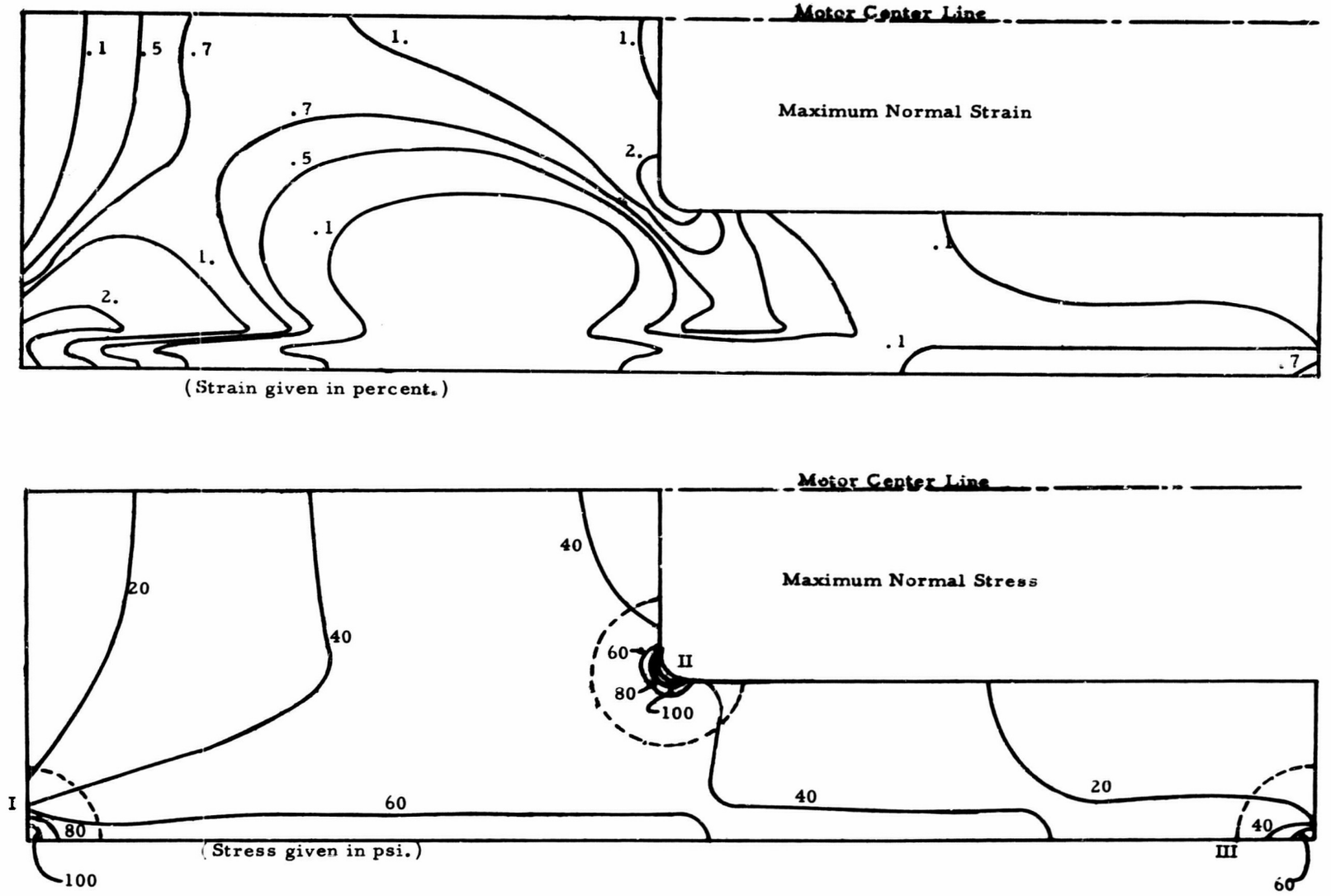


FIG. B-4 MAXIMUM NORMAL STRAIN AND MAXIMUM NORMAL STRESS DISTRIBUTION IN DUAL THRUST MOTOR SUBJECTED TO THERMAL SHRINKAGE LOADING (E = 1000 psi).

CONFIDENTIAL

only to indicate the distributions of the stresses and strains and not the magnitude of the extreme stresses and strains existing in the actual grain.

By examining Fig. B-4 is is apparent that there were three regions in the motor where stress (or strain) concentrations exist. These regions are indicated by the numerals I, II, and III. Normally, the magnitude of the stresses and strains at all these locations would be examined for possible failure conditions. However, since the conditions in Regions I and III are of the same character and since Region I is the most critical, only Regions I and II were considered in this analysis. Since changing the radius of the fillet does not alter the stress or strain distribution in Region I, only one basic configuration need be considered in determining the structural integrity of Region I.

The values predicted for the stresses and strains for the case of thermal shrinkage loading only in Region I are

$$\sigma_m \approx 53 \text{ psi}, \tag{B-1}$$

$$\tau_m \approx 24.8 \text{ psi, and} \tag{B-2}$$

$$\epsilon_m \approx 5.1\% \tag{B-2}$$

In Region II, the maximum stresses and strains predicted for the thermal shrinkage loading only for the three variations are summarized in Table B-I.

Table B-I

Thermal Shrinkage Loading Results for Region II

R (in)	ϵ_m (%)	σ_m (psi)
0.25	11.3	211.5
0.50	7.3	135.6
0.75	3.8	85.4

The failure conditions for the thermal shrinkage analysis can be determined from Fig. B-3 since for a cooldown time of 2 hours and a temperature of -40°F, the log of the reduced time can be found to be -2.721. For this reduced time, the maximum allowable stresses and strains can be found to be

$$\epsilon_{ma} \approx 16\%, \tag{B-4}$$

$$\sigma_{ma} \approx 100 \text{ psi, and} \tag{B-5}$$

$$\tau_{ma} \approx 50 \text{ psi.} \tag{B-6}$$

2. Pressurization Analysis

The head-end of the dual thrust grain is restrained from moving forward; hence, no shear deformation takes place in Region I due to pressurization. Since the stress condition there will be essentially hydrostatic, Region I was not considered in the analysis. Under pressurization, Region II would most likely be the location where failure conditions would exist.

To determine the correct modulus to use in this analysis, the reduced time must be computed. Assuming a pressurization time of 0.01 sec and a temperature of -40°F, the log of the reduced time was computed to be -8.58. Since the data available in Fig. B-1 does not cover this time span, a value of 25,000 psi was assumed for the modulus to be conservative in predicting the strains. The strains were assumed to be indicative of failure for the conditions being examined. As before, a bulk modulus of 350,000 psi was assumed.

The maximum normal stresses and strains determined in Region II for a pressurization loading are summarized in Table B-II.

Table B-II

Pressurization Results for Region II

R (in)	ϵ_m (%)	σ_m (psi)
0.25	21.6	600
0.50	14.0	451
0.75	8.0	353

The failure conditions under a pressurization load can be calculated in a similar manner as for the thermal shrinkage loading. The failure conditions are calculated for a pressurization time of 0.01 sec. For this time and a temperature of -40°F, the log of the reduced time is-8.58. Although, data is not available for a reduced time of this magnitude, the data available can be extrapolated to obtain the failure data if it is recognized that large errors may be introduced in the process. Extrapolating the curve in Fig. 3, the maximum allowable strain is estimated to be

$$\epsilon_{ma} \approx 1\% \qquad \text{(B-7)}$$

The maximum allowable normal stress is similarly estimated from Fig. B-3 to be

$$\sigma_{ma} \approx \log^{-1}(3.2) = 1580 \text{ psi.} \qquad \text{(B-8)}$$

Conclusions

Before any conclusions are made concerning possible failure conditions of the dual thrust motor, the limitations of the strength analysis need to be realized. In addition to the uncertainty caused by the small errors which result from use of the finite element method, there exist gross uncertainties regarding the appropriate failure criterion to use. At these Laboratories, the failure data is gathered only from uniaxial tests. Since this data must be interpreted in terms of possible failure conditions under multiaxial stress and strain conditions in the motor, large errors can be made in the process of predicting failure.

Under the thermal shrinkage loading alone, failure would most likely occur in Regions I and II. In Region I, failure would most likely occur by exceeding the shear stress of the bond causing the propellant to separate from the case. Since nothing is known of the bond strength in shear, the shear strength of the propellant alone must be utilized. The maximum shear stress predicted in Region I is given in

Eq. B-2 to be 24.8 psi. The maximum allowable shear stress is stated in Eq. B-6 to be 50 psi. This would seem to produce an adequate margin of safety regarding this feature.

In Region II, the maximum normal strain should probably be the limiting condition for the thermal shrinkage loading. By examining Table B-I, it can be seen that neither configuration A, B, or C produces strains which exceed the maximum allowable normal strain indicated in Eq. 4 to be 16%. Thus, failure in the fillet due to thermal shrinkage alone would be unlikely for any configuration examined.

In regard to the low temperature pressurization problem investigated, failure would most likely be a function of the maximum normal strain in the fillet. Since the strains listed in Table B-II for configurations A, B, and C exceed the maximum allowable strain of 1%, in Eq. 7, it seems very possible that failure would occur under the conditions examined.

In summary the dual thrust motor appears adequate in regard to bond failure at the head-end of the grain (Region I). In Region II, the indications are that failure is probable under pressure loading at low temperatures with the nitrocellulose plastisol propellant even with a 0.75-in. fillet radius.

APPENDIX C

TESTING OF NOZZLE THROAT INSERTS

Since the booster charge was designed to operate at a high pressure (~3000 psia) for 1.5 seconds, some tests were made early in the program to determine if standard graphite nozzle inserts would hold up under these conditions.

Two 6C3-6[1] plastisol propellant grains were modified to very nearly simulate the booster design by cutting three slots in one end and casting a head end web in the other end. The resultant charges were slightly shorter than the actual design.

The booster grain design performed very much as expected, but severe nozzle throat erosion caused low operating pressures. The throat areas enlarged approximately 40% during the tests. Graphite nozzle inserts were also tested at sustainer operating conditions with solid end-burning charges. No nozzle throat erosion occurred with the sustainer charges (Table C-I).

Table C-I

Tests on Graphite Nozzle Inserts Using Plastisol Propellant

Round No.	Propellant Charge	Pressure (psia)	Time (sec)	Nozzle Throat Diameter (in)	
				Before	After
4713	Booster	2065	1.8	0.496	0.600
4714	Booster	2256	1.7	0.498	0.592
4757	Sustainer	271	14.5	0.501	0.504
4758	Sustainer	261	14.3	0.502	0.505

A round was prepared to test a molybdenum throat insert with a complete booster and sustainer charge. This test utilized a 6C3-11.4[2] grain modified in a similar manner as the 6C3-6 except a full length sustainer charge was cast in the head end. The

[1] 6C3-6 designates a 3 inch ID cylindrically perforated propellant charge in a 6 inch ID by 6 inch long motor case.

[2] A 3 inch ID cylindrically perforated propellant charge in a 6 in. X11.4 in. motor case.

actual operating conditions of the dual thrust motor were simulated in this test, and the molybdenum throat insert was not eroded.

APPENDIX D
OPTIMIZATION OF NOZZLE EXPANSION CONE

Three nozzle designs were considered for the dual-thrust motor.

1. A separating exit cone design permits optimum expansion and thus maximum impulse for both the booster and sustainer operations. However several inherent disadvantages render this design unattractive for tactical field weapons. The separating exit cone generates a falling object early in its trajectory which in many applications could be a hazard to troops deployed along the missile flight path. The separation mechanism and initiator significantly increases the cost and complexity of the motor hardware and decreases the operation reliability. A maximum gain of 5% total impulse could be expected with a separating exit cone when compared to a fixed expansion ratio nozzle, but a 4% addition in hardware weight would be required. This design was rejected.

2. The step nozzle designs attempts to provide full expansion at booster pressure and to control the overexpansion of the sustainer gases by providing a sharp separation point (Fig. D-1).

The concept was tested by sixteen firings of 2C1.5-4 clamp motors. One series of motors operated at 200 psia chamber pressure to simulate the sustainer conditions, and one series operated at 3200 psia to simulate the booster conditions. RH-P-163cc propellant was used in the sustainer motors and RH-P-163-cb propellant was used in the booster motors. Four different test configurations were fired; sustainer control, sustainer step, booster control and booster step. (Figs. D-2, D-3). The control nozzles were of the conventional optimum expansion ratio design. The results show the step nozzle to be from 5.4% to 6.9% less efficient than the control rounds (Table D-I).

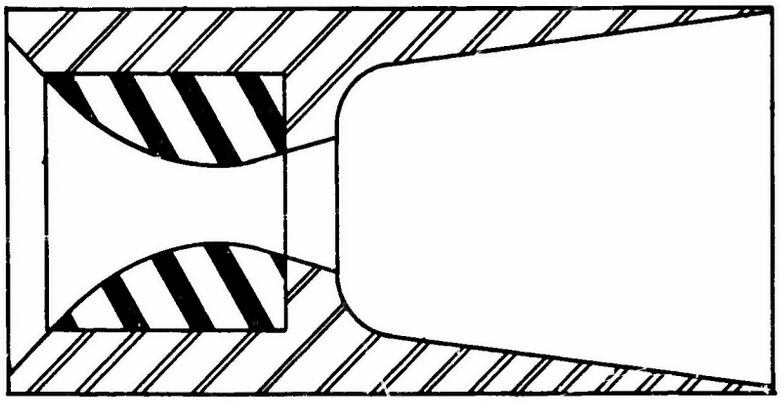
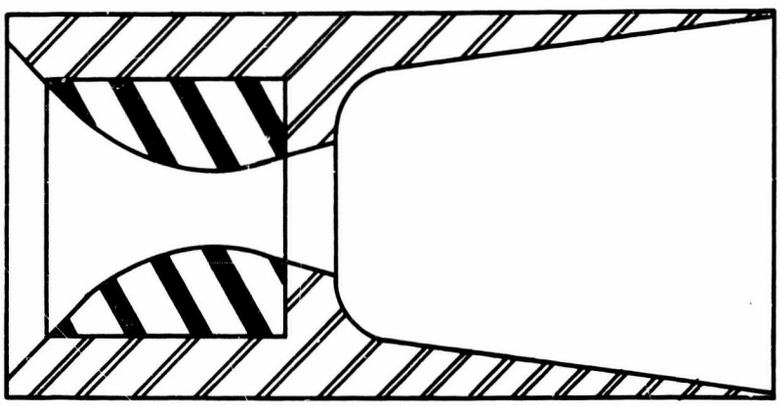
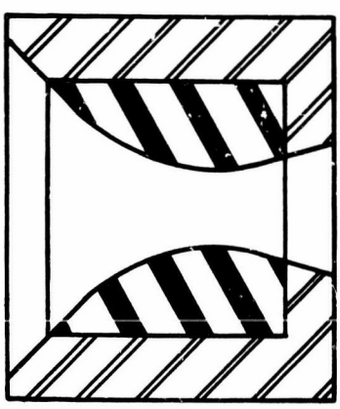


FIG. D-1 STEP NOZZLE CONCEPT.

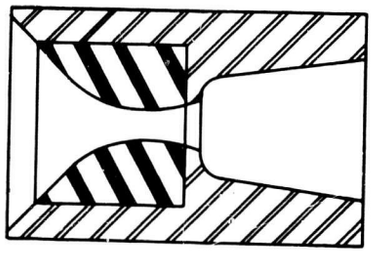


SUSTAINER STEP NOZZLE

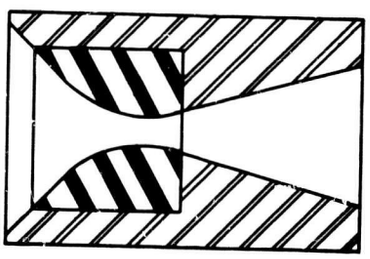


SUSTAINER CONTROL NOZZLE

FIG. D-2 SUSTAINER TEST NOZZLES.



BOOSTER STEP NOZZLE



BOOSTER CONTROL NOZZLE

FIG. D-3 BOOSTER TEST NOZZLES.

3. The fixed expansion ratio nozzle offers the greatest simplicity of manufacture and least weight of the designs considered. A computer program was prepared to optimize the fixed expansion ratio for maximum total performance for the dual thrust motor. An expansion ratio of 5.45 was found to provide theoretical values of 999 lbf booster thrust and 51.4 lbf sustainer thrust with the grain design selected for the dual thrust motor. 94.4% of maximum possible combined total impulse should be obtained with the 5.45 expansion ratio nozzle compared to 93.7% for the step nozzle design.

From the nozzle design considerations, the 5.45 fixed expansion ratio nozzle was selected for the dual thrust motor test program.

Table D-I

Variations in Thrust Coefficient Between Step Nozzles and Control Nozzles

Round No.	Nozzle Type	Average Chamber Press. (psia)	C_F	$C_{F(1000)}$
4717	sustain control	197	1.2148	1.4800
4718	sustain control	195	1.2199	1.4922
4719	sustain control	188	1.2175	1.4964
4720	sustain control	198	1.2215	1.4880
Average values		195	1.2184	1.4891
4721	sustain step	199	1.1647	1.4191
4722	sustain step	178	1.1303	1.3989
4723	sustain step	201	1.1438	1.3902
4724	sustain step	190	1.1670	1.4308
Average values		192	1.1515	1.4098
% Diff. between sustain step, sustain control			5.5	5.4
4725	boost control	3250	1.5825	1.4940
4726	boost control	3364	1.5918	1.4997
4727	boost control	3328	1.5909	1.4976
4728	boost control	3089	1.5918	1.5078
Average values			1.5893	1.4998
4729	boost step	3141	1.4654	1.3866
4730	boost step	3213	1.4978	1.4147
4716	boost step	3016	1.4735	1.3969
4766	boost step	3017	1.4597	1.3848
Average values			1.4741	1.3957
% Diff. between boost step and boost control			7.3	6.9

APPENDIX E

ANALYSIS OF PRESSURE LEVEL OF SUSTAINER OPERATION WHEN A SIGNIFICANT MASS OF LINER BURNS

The continuity equation where no contribution from liner is realized is written as

$$\rho S c P^n = C_{D_1} A_t P \qquad \text{(E-1)}$$

where

ρ = propellant density = 0.058 lbm/in^3

S = propellant surface area = 25.60 in^2

c = burning rate constant = 0.0151

P = chamber pressure, psia

C_{D_1} = discharge coefficient = 0.0063 lbm/lbf-sec

A_t = nozzle throat area = 0.2428 in^2

n = pressure exponent = 0.485

Rearranging (E-1) gives

$$P = \left(\frac{\rho S c}{A_t C_D}\right)^{\frac{1}{1-n}} = 175 \text{ psia} \qquad \text{(E-2)}$$

which is the pressure for normal sustainer operation.

Including the liner contribution in the continuity equation gives

$$\rho S c P^n + \dot{m}_\ell = C_{D_2} A_t P \qquad \text{(E-3)}$$

where $\dot{m}_\ell$ = mass discharge rate of liner = 0.043 lbm/sec and C_{D_2} = effective discharge coefficient during sustainer operation = 0.0068 lbm/lbf-sec.

Rearranging (E-3) gives

$$P^n \frac{\rho S c}{A_t C_{D_2}} + \frac{\dot{m}_\ell}{A_t C_{D_2}} = P \qquad \text{(E-4)}$$

which, solved by trial and error, gives

$$P = 208 \text{ psia} \qquad \text{(E-5)}$$

These relations show a 33 psi increase in pressure due to burning of the liner.